Article:
Broekaert, J.B., Hancock, T.O., Hafiz, F. et al. (2026) Deciding by quantum-like belief morphing or hopping?Its application to multi-agent response influence. Journal of Mathematical Psychology, 130. 102994. ISSN: 0022-2496

https://doi.org/10.1016/j.jmp.2026.102994

Deciding by quantum-like belief morphing or hopping? Its application to multi-agent response influence

Jan B. Broekaert[a,*], Thomas O. Hancock[b], Faizal Hafiz[a], Stephane Hess[b], Davide La Torre[a]

[a]SKEMA Business School, Université Côte d'Azur, Sophia Antipolis, France
[b]Choice Modelling Centre & Institute for Transport Studies, University of Leeds, United Kingdom

Abstract

Other people's beliefs may influence our own. Such effects, sometimes referred to as 'crowd-wisdom', can be revealed from group-informed responses in controlled experiments. Our study presents a formal choice model to understand how multiple respondents iteratively interact when communicating their responses, which we test on data from Granovskiy et al. (2015)'s social information experiment. In this multi-stage decision process, information from the group's response distribution influences individual judgments before respondents adjust their next response. Our model describes each respondent's probabilistic belief state, and uses a quantum-like morphing evolution based on the Brassard-Høyer-Grover amplification formalism. This framework enables: (i) the description of multi-respondent cognitive interactions through assimilation to or polarization away from other beliefs, (ii) the implementation via Hamiltonian operators using projection operators of *source* ('initial') and *target* ('informing') belief states, and (iii) the resolution of periodicity issues in previous Schrödinger-like

*Corresponding author
Email addresses: jan.broekaert-ext@skema.edu (Jan B. Broekaert), T.O.Hancock@leeds.ac.uk (Thomas O. Hancock), faizal.hafiz@skema.edu (Faizal Hafiz), S.Hess@leeds.ac.uk (Stephane Hess), davide.latorre@skema.edu (Davide La Torre)

models through bounded temporal parametrization. A performance comparison is done for the quantum-like models using *morphing* and standard *hopping*, and a classical Markov hopping model. The quantum-like morphing model with multi-component target belief demonstrated superior BIC performance across the parameter space of evolution time (t_{frac}), belief uncertainty (SD), and sampling temperature (T). This belief morphing approach hence provides an effective and innovative method to model social influence in group decision-making.

Keywords: Quantum-like cognition, Brassard-Høyer-Grover amplification, crowd-wisdom

---

1. Introduction: quantum-like cognition

Processing perceived social information can be a challenge; innate and acquired information aggregation heuristics can either align one's beliefs with effective crowd wisdom or, conversely, amplify one's uncertainty on the issue at hand. This, in turn, makes it unsurprising that *rational* decision models that incorporate a perceived spread of contextual information and a respondent's own uncertainty have often produced predictions that differ from respondents' observed decisions.

Human decision-making frequently deviates from the prescriptions of classical rationality, even in the absence of external influence. Extensive empirical research has revealed systematic patterns in which individuals violate the axioms of classical logic, probability theory, and expected utility theory. The seminal work of Herbert Simon included bounded rationality to outline operational administrative behavior that aims to be as goal-efficient as possible, but is limited by systemic and practical unknowns (Simon and Barnard, 1947). As famously pointed out by Maurice Allais, a behavioral paradox countering classical utility theory shows that people—through lottery experiments—will incorporate the effect of an irrelevant "zero"-lottery to inconsistently switch preferences between contrasted lottery options (Allais, 1953). The work of Edwards brought subjective Bayesian probability into decision making and noted the under-accommodation of evidence in effective judgment. For example, blue/red mixed-chip experiments show that people conservatively update their beliefs about the mix ratio 'too slowly' in comparison to Bayesian updating (Edwards et al., 1963). Daniel Ellsberg complemented the observations of Allais with behavioral ambiguity aversion (Ellsberg, 1961). These logical violations are not merely occasional errors but robust, replicable phenomena that challenge the foundational assumptions of traditional economic and decision-theoretic models. More recent behavioral researchers-cognitive psychologists Daniel Kahneman, Amos Tversky, and Eldar Shafir, and behavioral economist Richard Thaler-have documented numerous cognitive biases and decision paradoxes—such as the conjunction fallacy, framing effects, and violations of the sure-thing principle—that expose the limitations of classical probability frameworks in describing human cognition (Kahneman, 2011; Tversky and Shafir, 1992; Shafir and Tversky, 1992; Thaler and Johnson, 1992). The ubiquity of these phenomena demonstrates the necessity of developing alternative formal frameworks capable of accommodating these characteristic features of human judgment and choice. It is within this context that quantum-like approaches to cognition have emerged as promising candidates for modeling decision processes that classical frameworks cannot adequately capture. The discrepancy between one's own beliefs and the beliefs of others involves assessing one's proper adeptness and rational grounds for a given answer and reflecting on external information, and more intuitive and emotional effects induced by the group's multiple answers. The effect of self vs other, the effect of confirmation vs refutation, and congruous vs dispersed signals, all contribute to the uncertainty in integrating crowd information. While such integration is often modeled as a rational, logic-based cognitive process, a quantum-like formalism can also capture the contextual uncertainty and bias effects that arise when processing crowd responses.

Quantum-like approaches in behavioral science apply quantum formal principles and probability structure, without assuming that quantum physical processes in the brain are the underlying mechanism. In cognitive science, their application focuses mainly on functional models over neurophysiological brain processes.[1] These models apply selected formalism from the mathematical framework of quantum mechanics to cognitive processes, suggesting similar processes in human cognition (Pothos et al., 2021; Busemeyer and Bruza, 2012). These approaches may accommodate decision-making settings where the use of classical probability leads to inconsistent inferences or to paradoxical deduction. There are several well-known examples of these, including the conjunction fallacy, when a decision-maker judges the probability of two events occurring together as higher than each

[1] Attempts to effectively model cognitive processes in the brain through quantum mechanics can be found in the work of Hameroff and Penrose (2014), or e.g. Khrennikov et al. (2025).

one alone, as in the case with the "Linda feminist-bank-teller problem" (Tversky and Kahneman, 1983). A second example is the ordering effect, when responses are changed based on their position in a sequence, as in the electability of "Clinton-then-Gore vs Gore-then-Clinton" (Wang et al., 2014b; Trueblood and Busemeyer, 2011). A third example is the disjunction fallacy, which implies violating the sure-thing principle by misjudging a decision on an encompassing event while its sub-cases are oppositely judged, as in only stopping a proposed gamble under the condition that a previous gamble outcome is unknown - i.e. 'won or lost' (Tversky and Shafir, 1992). These decision-making settings all require judgments from a decision maker, which can be influenced by the settings themselves. The implementation of belief states is the essential characteristic of quantum-like models that enables these phenomena to be captured. These states are represented by vectors that contain the complex probability *amplitudes* for each *observable* in their corresponding vector components. Their superposition, entanglement, and collapse by measurement, enable to capture the cognitive idiosyncrasies of these processes, but ubiquitously, also other non-classical probabilistic outcomes in various systems (Khrennikov, 2010, 2023; Aerts et al., 2016; Bagarello, 2019). In these models, responses are considered *realized*, not *revealed*, by measurement –prior to which these decisions of a respondent remain potential (Lambert Mogiliansky et al., 2009). The process of sequential sampling of evidence prior to decision making that is regularly accommodated in classical models (Smith and Ratcliff, 2015; Diederich and Busemeyer, 2003) can also be included in quantum models (Busemeyer et al., 2009; Epping and Busemeyer, 2023), particularly by a process of diffusion over *trust* or *action* levels for responding. The respondent's newly sampled evidence translates into evolving probabilities –or amplitudes– to support or reject their decision. The Kolmogorov-forward equation and the Schrödinger equation enable these respective paradigms to model the changing believes or trust and support for specific decisions in a task. The operators of change in these models are respectively the Markov transition rate matrix, and the Hamiltonian operator (Busemeyer and Bruza, 2012).

Our current study adapts the aim and the underlying belief dynamics: a responder is informed about the responses of other responders –on the same task– and subsequently aims to adjust her or his own response, or not. Our model will be implemented here specifically for group-influenced decision-making, as in the setting of Granovskiy et al. (2015)'s study. In this configuration, the basic premise of the Hamiltonian dynamics is to make one's original belief state evolve towards a new response in a controlled way by other's belief states, or not. Technically, we will adapt Grover's amplification algorithm into a *morphing* dynamics for belief states (Brassard and Høyer, 1997; Grover, 1998). The belief state *morphing* approach has some merits. The structure of the morphing Hamiltonian –formally defined in Section 4, Eq.(5)– is easily interpretable. No direct designing at the component-level of the Hamiltonian needs to be done. Essentially, the respondent's initial belief state and a designed target belief state make up the morphing Hamiltonian through their projectors. The design of the target state follows from factors present in the choice-making setting and implements the interpretable parameters directly. This contrasts the component-wise construction in which the summation of weighted Hamiltonians may not necessarily correspond effectively to *combined* cognitive effects (e.g. one component for *utility* and another for *ambiguity*, see Broekaert et al. (2020)). In applications, the targets could either represent parameterless 'ideals', or be constructed as parametrized states with distinct interpretations (see Section 7).

An additional advantage of the morphing approach is that it provides an unambiguous interpretation of the temporal evolution of the state vectors, in particular its inherent periodicity. In the component-wise Hamiltonian construction method, the recurrence period can only be derived implicitly, whereas in the morphing method, the (half) recurrence period is explicitly determined by the inner product of the source and target states. The amplitude of the evolution parameter - previously designated as Schrödinger's *temporal ordering* parameter (Aerts et al., 1999; Broekaert et al., 2006; Broekaert and Busemeyer, 2017) - now acquires the characteristic of a *utility* function of the target belief state for the decision maker. The belief state morphing approach is hence an effective way to address the *periodicity* of the Schrödinger-like dynamics for cognitive modeling. The quantum-like description with Schrödinger-type evolution entails periodic behavior, a natural property in an energetically closed system, referred to as Poincaré recurrence (Bocchieri and Loinger, 1957), but not expected for a human belief state –except for some rare circumstances involving self-reference (Aerts et al., 1999; Broekaert et al., 2006). The well-defined finite state morphing period sets a limit to the window of the evolution parameter and thereby enables to avoid repeated approximate recurrences with variations due to limited computational precision.[2]

The presentation of the quantum-like belief morphing model in our paper is structured as follows. In Section 2, a focused literature review is given of dynamical or Hamilton-based quantum-like approaches. To introduce the basic quantum formalism for cognition, Section 3 –on current quantum-like methodologies, reviews and explains the necessary formal concepts. The main contribution in this study is the novel belief state *morphing* approach, and is presented and developed in Section 4, 'Belief state morphing dynamics'. To test the performance of the morphing approach, another new quantum-like competitor based on a *hopping* formalism is presented in section 5, this approach also allows to infer a corresponding classical-logic-based Markov model. In the crowd-wisdom experiment focused Section 6, the social-influence experiment by Granovskiy et al. (2015) is discussed. It serves as the paradigm for repeated belief morphing. Then, potential target beliefs in group decisions are devised in Section 7 focused on the adaptation of the morphing formalism to social influencing. Also a method to account for inter-subject differences in individual responses is developed, using Gumbel random sampling. In the results Section 8, the performance of the quantum-like and classical models are tested and compared on the Granovskiy dataset. The conclusions are presented in Section 9. Supplementary material on the formal resemblance of the Schrödinger and Markov dynamics appears in Appendix A, aspects of the Granovskiy dataset are described in Appendix B, morphing *in opposition* or with complex

[2]Numerical simulations of q-like systems at finite precision (e.g. float64) necessarily lead to pseudo-periodicity.

tree-structured targets is formulated in Appendix C, and Gumbel sampling is described in Appendix D.

2. Context and literature review

To measure is to disturb, perchance to create the response instead of discovering it –a persistent conundrum for measurement-based statistics in psychological studies of decision processes, and a central tenet to quantum probability theory (Aerts and Aerts, 1995; White et al., 2014). Quantum-like models have consequently been used to address phenomena where classical probability theory is challenged to explaining paradoxical human decision-making, context-dependent judgments, cognitive biases, e.g. conjunction and disjunction effects, or response discrepancies from switched question order (Aerts and Gabora, 2005; Busemeyer et al., 2006a; Khrennikov, 2010; Wang et al., 2014a). A variety of approaches have been developed: complementarity-based Hilbert space representations with basis transformations for each change of cognitive perspective, Hilbert space projections for the belief state collapse for decisions taken, and state entanglement for the composition of concepts or actions, with polysemous meaning or contextual activation (Busemeyer and Bruza, 2012). The context of our present study are the dynamical approaches that aim to describe the change of belief states over 'time'.[3] The Schrödinger-like evolution enables to model changing believes or trust or support for specific decisions in a task. In particular, the Hamiltonian, as the operator of change, holds pa-

[3] In quantum theory of energetically closed systems, *time* is essentially reversible and evolution is periodical, see Section 3.

rameters to reinforce, diminish, and mix specific components of belief. The parameters can be cooperate-defect utility based (Pothos and Busemeyer, 2009; Eisert et al., 1999), ambiguous observation related (Atmanspacher et al., 2004) logic-inference based (Aerts et al., 1999; Broekaert et al., 2006), gist-verbatim based (Broekaert and Busemeyer, 2017, 2019), categorization-decision mixed (Wang and Busemeyer, 2016; Zheng et al., 2023), win-loss utility informed (Broekaert et al., 2020), relate to explanatory factors of a choice setting such as journey characteristics(Hancock et al., 2020b,a), or strategic interaction induced (Martínez-Martínez, 2014). Open system dynamics with Lindblad evolution have also been used to mitigate the periodic behavior in Schrödinger approaches. Specifically, response-time paradigms require the open system's Lindblad-type governing equation under which belief states evolve long-term to a damped oscillatory regime (Asano et al., 2011a; Epping et al., 2023; Khrennikov, 2023; Asano et al., 2011b; Khrennikova et al., 2014; Martínez-Martínez and Sánchez-Burillo, 2016; Kvam et al., 2015; Rosner et al., 2022). Invoking second-quantization, Bagarello (2019) constructs cognitive models in a Fock-like occupation-number space in which discrete cognitive quanta flow between states, and non-Hermitian extensions of the Hamiltonian –for the gain or loss of quanta from an environment– result in open-system dynamics. Belief morphing has in common with quantum-like Bayesian updating a posterior state following a contextual exposure of a prior state. Brody (2023) implements a dynamics of Bayesian information acquisition by iterated Neumann–Lüders updating, as it minimises uncertainty while remaining consistent with the measurement outcome state. Morphing does not incorporate *per se* a logic-based updating of a belief state, any idiosyncratic influence by an exposure is possible. In experimental paradigms like Granovskiy et al. (2015)), where physical response times are not recorded and only ordered rounds are observed to perform tasks correspond, a bounded unitary evolution suffices to capture belief change. In contrast, in tasks with response-time distributions or repeated oscillatory responses over time, the open-system approach is the more appropriate setting.

The morphing dynamics approach presented here shares with *quantum reinforcement learning* the basic principle of inferring a target belief state. In an exploration-exploitation balanced strategy, a stepwise alteration of the belief state is adopted depending on its improvement of a prediction or reward (Busemeyer and Bruza, 2012). Grover quantum reinforcement learning, developed by Dong et al. (2008), was proposed in a grid world task of navigating to a goal while avoiding penalties from obstacles. This approach was adapted by adding a reward function from partial observations (Jiang et al., 2022). Similarly, the method was implemented for a networked quantum associative memory (**?**), and developed to explain the availability bias in which probability estimates are erroneously based on how easily cases can be recalled (Franco, 2009). The method was empirically tested in subjects performing the Iowa Gambling Task and correlated with medial frontal gyrus variables (Li et al., 2020). An amplitude amplification underlies the choice rule for assigning probabilities to actions in a simulated predator-prey grid world (Fakhari et al., 2013; Rajagopal et al., 2021).

In belief state *morphing*, the evolution process is governed by a continuous-time equation based on the Brassard-Høyer-Grover amplification formalism

(Grover, 1996; Brassard and Høyer, 1997; Grover, 2001; Roland and Cerf, 2003). While the amplification algorithms have been devised for fast searching the oracle-tagged output (by flipping its complex phase), integrating the underlying dynamics yields an 'analog analogue' evolution of hybrid states between an original *source* and a *target* belief state (Farhi and Gutmann, 1998).[4] Our morphing approach essentially presents a generalization of this gradual source-target state transition.

In a different dynamic approach, a source-target transition can be devised in which e.g. belief states with *intermediate* response values are held. In this perspective, and adapted to the experimental paradigm in our study, a quantum *hopping* model with step-ladder-like dynamics over the *response-value* range is devised (Hubbard, 1963; Feller and Livine, 2017). This approach hence differs from the sequential evidence sampling approach by quantum diffusion dynamics that aim to evolve the *confidence* level of a response (Diederich and Busemeyer, 2003; Busemeyer et al., 2009; Kvam et al., 2015). Finally, other recent quantum-based models for group decision making have shown that reaching a consensus could be prone to interference effects from individual subjective beliefs (Jiang and Liu, 2022), or that collective motion emerges from mutual visual perception (Beuria et al., 2025). This type of interference is present in our model as well in, e.g., target states that compound other participant responses by superposition (see Section 7). The next section will provide a brief presentation of the

[4] A continuous time integration of the Grover search problem by Farhi and Gutmann (1998) relates the *continuous* (or 'analog') search time to the size, N, of an unsorted list, and was hence coined an 'analog analogue' result.

quantum-like method to accustom the reader to just the required basic concepts and formalism.

3. Quantum-like models for decision making

To implement a quantum-like process in cognitive modeling, an adaptation and simplification of the quantum mechanical formalism are required (Busemeyer and Bruza, 2012; Khrennikov, 2010; Yearsley, 2017; Yearsley and Busemeyer, 2016). In practice, the dimensions and features of the model are set by the measured properties, the operational order of the experimental paradigm, and theoretical presuppositions. In a quantum-like model, the belief-action state is represented by a vector in a Hilbert space, which is a regular vector space with an inner product and a completeness property which assures limits will exist. In most cognitive models this space will be the finite-dimensional complex-valued space $\mathbb{C}^n$, and its vectors $\psi = (\psi_1 \dots \psi_j \dots \psi_n)$, with respect to the origin, represent a belief-action state for n properties. These states are often denoted in bra-ket notation as a column vector $|\psi\rangle$, or complex-transposed as a row vector $\langle\psi|$. For example, in the considered experimental paradigm (Section 6), a participant i, with revealed decision value in the first round R_{1i}, $R_{1i} \in [0, 100]$, will be allocated a belief state that is concentrated about this response value. Specifically, a (truncated) Gaussian will be allocated with mean R_{1i} and spreading over the full range of possible response values, Eq.(16). The response of a participant is a measurement outcome for a given property, which occurs by a measurement enacted by a measurement operator. The probability p_k of a given outcome value k is obtained by applying the projector M_k, spanned by the eigen-vector for response k, on the belief state $|\psi\rangle$ and taking the norm squared:

$$p_k = ||M_k|\psi\rangle||^2 = \langle\psi|M_k|\psi\rangle \tag{1}$$

This is the conventional Born's rule for outcome probabilities in quantum mechanics. The belief state $|\psi\rangle$ of a participant changes over time by cognitive input through the cues in the experimental paradigm. As mentioned, the Schrödinger equation is used to capture the dynamic process for this cognition evolution, and needs 'temporal' constraining for its periodic behavior. In other 'time-less' quantum-like models that emphasize complementarity of features, this evolution is abstracted and ad hoc unitary matrices are used to propagate the belief-action state (Aerts, 2009). In the Schrödinger approach, a temporal parameter, 'time' t , orders the subsequent belief-action states, and evolves them according to the Hamiltonian operator:[5]

$$i\frac{d}{dt}\psi(t) = H\psi(t). \tag{2}$$

It is hence the precise make-up of this fundamental operator of infinitesimal change, H, that delivers the tried-and-tested evolution in the quantum sphere. In particular in a finite-dimensional space (e.g. response values 0 to 100), the corresponding Schrödinger equation is simply satisfied through

[5]For finite-dimensional cases, the partial differential towards time becomes the total derivative. Also, Planck's constant, which is the unit of action, was set equal to 1. This renders both the 'energy' and 'time' into dimensionless variables.

matrix multiplication of the initial state with the unitary transformation U_t

$$\psi(t) \;=\; U_t\psi(0)\;, \;\text{ with }\; U_t = e^{-iHt}. \tag{3}$$

Central to developing a quantum-like model is therefore the construction of the Hamiltonian operator, since its components must direct the transfer of probability amplitude in line with cognitive theoretical principles that are applicable in a given task context.

Energy conserving or *closed* systems expose *Poincaré recurrence* or cyclic behavior. Here, time functions as a temporal ordering parameter. Only in energetically *open* systems does the time parameter correspond to macroscopic –'thermodynamically oriented'– time. Theoretically a period τ exists for which, $\psi(0)$=$e^{i\varphi}\psi(0+\tau)$, or 'each belief state is recurrent over time'. This characteristic needs to be monitored when numerical fitting to observational data is done. Choice or judgment prediction by Hamiltonian methods need the evolution to be contained within the period τ of the system: each state reached beyond this period is merely an identical repetition from the previous cycle. To derive the system's period, it is noted an n-dimensional Hamiltonian will have at most n real eigenvalues, less when degeneracy occurs. The spectral decomposition of the Hamiltonian $\{E_j\}$, in an orthogonal basis, $\{\mathscr{E}_i\}$, and the unitary operator, $\sum_j e^{-iE_jt}P_{\mathscr{E}_j}$, points out the system's periodicity. For a pre-defined accuracy of energy –unit e_{acc}– the spectral energy levels E_j can be expressed as integer multiples $E_{j,\text{acc}}$ of the energy unit. This implies that the unitary operator at time t –e.g. at t=0, the unit matrix– is exactly reproduced up to irrelevant relative phase differences of

2π at time $t+\tau$. The period of the system is

$$\tau = \frac{2\pi}{GCD(\{E_{j,\mathrm{acc}}\})}, \tag{4}$$

where $GCD(\{E_{j,\mathrm{acc}}\})$ is the greatest common divisor over the approximated set $\{E_{j,\mathrm{acc}}\}$, or their prime decompositions.[6] In the next section a similar bound on evolution time will be derived for morphing dynamics.

4. Belief state morphing dynamics

Belief state morphing is a quantum-like approach that describes how to evolve one given belief into another. It aims to describe how the decision-making setting influences a prior belief—or "source" state—into a posterior belief—or "target" state. The core algorithm of belief state morphing is the unitary one-parameter group, Eq.(3), now devised to evolve two pre-defined state vectors –parameterized to capture the properties and effects of the decision-making setting– into each other. In line with the continuous-time analog of the Brassard-Høyer-Grover amplification formalism of the oracle state (Brassard and Høyer, 1997; Grover, 1996, 2001; Roland and Cerf, 2003), the (analog) Hamiltonian of Farhi and Gutmann (1998) is adapted here to implement this general scheme of morphing between any two non-orthogonal belief states.

The morphing evolution between two belief states ψ_A and ψ_B, is realized by

[6]E.g., if the eigen energies would be $\{51.234.., 10.756.., 4.201..\}$, and the accuracy set to e_{acc}=.1, then the set is expressed as $\{512, 108, 42\}$, or in prime decomposition $\{2^9, 2^2 3^3, 2\cdot 3\cdot 7\}$, with a GCD=$2^9 3^3 7$ and period τ=$\pi 2^{-8}3^{-3}7^{-1}$.

setting the Hamiltonian according to:

$$H = \mathcal{I} - P_{\psi_A} - P_{\psi_B}, \qquad {P_{\psi_\bullet}}^2 = P_{\psi_\bullet}, \tag{5}$$

where P_{ψ_A} and P_{ψ_B} are the projectors on the respective states, and $\mathcal{I}$ is the identity operator. The connection to Grover's algorithm lies in the use of a Hamiltonian built from projectors on the initial and 'oracle' (target) states, which generates amplitude amplification in a low-dimensional subspace spanned by source and target, as in continuous-time analogs of Grover's search (Farhi and Gutmann, 1998). In contrast, our morphing scheme does not perform search over an unknown marked item but reinterprets a similar mathematical mechanism as a controlled interpolation between prior and target belief states, with the 'oracle' replaced by psychologically motivated target beliefs. The morphing dynamics can therefor be regarded as a cognitive reinterpretation of a Grover-type amplitude amplification rather than a literal implementation of Grover's algorithm.

The analytical expression of the evolved state $\psi_A(t)$, or $\psi_B(t)$, is obtained from the Taylor expression of the unitary propagator $e^{-iHt} = \sum_{k=0} \frac{(-it)^k}{k!} H^k$, where t is the evolution parameter (Appendix C). Defining the shared belief amplitude between both states

$$\lambda \coloneqq \rho_{AB} e^{i\theta_{AB}} \coloneqq \langle \psi_A | \psi_B \rangle, \tag{6}$$

with modulus $\rho \in [0, 1]$ and complex phase $\theta \in [0, 2\pi]$, the operation of H on the initial state ψ_A yields;

$$H\psi_A \;=\; -\lambda^\star\psi_B, \quad \text{and} \quad H^2\psi_A \;=\; |\lambda|^2\psi_A. \tag{7}$$

The state $\psi_M(t) = U(t)\psi_A$, evolving from the source state ψ_A can then be expressed as

$$\psi_M(t) \;=\; \psi_A \sum_{k=0} \frac{(\text{-}1)^k t^{2k}}{(2k)!}|\lambda|^{2k} + i\frac{\lambda^\star}{|\lambda|}\psi_B \sum_{k=0} \frac{(\text{-}1)^k t^{2k+1}}{(2k+1)!}|\lambda|^{2k+1}, \tag{8}$$

or trigonometrically

$$\psi_M(t) \;=\; \cos(\rho_{AB}t)\psi_A + ie^{\text{-}i\theta_{AB}}\sin(\rho_{AB}t)\psi_B. \tag{9}$$

The dynamics, resulting from H, Eq.(5), will hence render the initial belief state ψ_A into the final belief ψ_B at $t{=}\frac{\pi}{2\rho_{AB}}$, and will at all times keep a weighted superposition of both belief states. For intermediate t, both components are present with a relative phase, which will produce interference when probabilities are computed in other bases or for composite targets.
Interpreting this as a *morphing* dynamics from a *source* into *target* state, the amplitude of the evolution parameter t is an indicator of the significance of the adopted belief change. Defining the full morphing period and the evolved fraction;

$$\tau_{AB} \;=\; \frac{\pi}{2\rho_{AB}} \quad , \quad t_{\text{frac}} \;=\; \frac{t}{\tau_{AB}}. \tag{10}$$

The morphing dynamics will produce a hybrid belief state between the origin state ψ_A for t_{frac}=0, and the target ψ_B for t_{frac}=1, the latter more precisely with an inconsequential overall complex phase $ie^{-i\theta_{AB}}$, see Fig.1.[7] The amplitude of the evolution parameter t_{frac} reveals the extent to which the respondent values adjusting their response w.r.t. the target. E.g., if t_{frac}=0.3, the respondent has morphed 30% of the way toward the target belief state. The morph period τ_{AB} for the evolution parameter is required to fully adopt the target belief. Intuitively appealing –and conform to the original Grover search algorithm– the full morph period τ_{AB} is larger when the initial belief state has less overlap with the target belief state. The amplitude of the evolution parameter –in practice the fraction t_{frac} of the τ_{AB} period– expresses the utility or valence of the targeted cognitive state, with respect to the current cognitive state. If the fraction t_{frac} is small, the respondent does not value much the change of mind, and barely morphs, when the fraction is closer to 1 it means the responder strongly adheres to the target belief, perceiving the utility of the target belief.

The morphing approach uses the expressions of a source and a target state to construct the Hamiltonian, in contrast to devising a utility function for each entry H_{ij} of the Hamiltonian. For complex belief-states, the morphing approach can provide a simpler construction even when multiple underlying intentions need to be included (see Appendix C). Besides the more transparent composition of the Hamiltonian, also the range of the (temporal) evolution parameter - or the intensity of change - is interpreta-

[7]The overall complex phase $ie^{-i\theta_{AB}}$ does not alter the properties derived from the belief state, since strictly a quantum state is described by the *ray* of the vector, see e.g. Weinberg (1995)

tively clear given its *ab initio* fixed range of possible values.

We remarked, from Eq.(6), that morphing between states is mathematically not possible when these are orthogonal to each other: when belief overlap $\rho=0$ their morphing period becomes infinite, Eq.(10). A direct transformation between states hence requires $\rho\neq0$, but also a auxiliary bridging vector with non-zero intersections at both ends could otherwise be introduced for a two-component target morphing scheme, Appendix C. Fitted belief vectors in cognitive models are almost never assigned zero amplitudes to any of their components. In cognitive terms, this means that there is always some residual probability associated with alternative choices, even when these alternatives are mutually exclusive. It has been observed that cognition tends to allocate a small but nonzero probability mass to opposing beliefs in orthogonal states (Basieva et al., 2017). Examples include the 'attack' vs 'withdraw' decision in categorization-decision tasks (Busemeyer et al., 2006b; Zheng et al., 2023), the 'gamble' vs 'stop' choice in conditional decision tasks (Broekaert et al., 2020), the differentiation among 'list 1', 'list 2', and 'list 3' in episodic memory source recall (Broekaert and Busemeyer, 2017, 2019), the 'front view' vs 'back view' perception in the Necker's cube (Atmanspacher et al., 2004), the 'true' vs 'false' evaluation in the Liar Paradox (Aerts et al., 1999; Broekaert et al., 2006), and the 'defect' vs 'cooperate' strategy in the prisoner's dilemma (Pothos and Busemeyer, 2009). These Hamiltonian-based models could hence be cast along the morphing approach as well. In particular, this approach will apply the morphing propagator–derived in Appendix C

$$U(t) = e^{-it} + \frac{1}{1-|\lambda|^2}\{P_{\psi_A}, P_{\psi_B}\}\left(e^{-it} - \cos|\lambda|t + \frac{i}{|\lambda|}\sin|\lambda|t\right) - \frac{1}{1-|\lambda|^2}(P_{\psi_A} + P_{\psi_B})\left(e^{-it} - \cos|\lambda|t + i|\lambda|\sin|\lambda|t\right) \quad (11)$$

between key identifiable cognitive states, ψ_A and ψ_B, of an experimental paradigm.[8] The anti-commutator of the projectors is denoted by curly brackets, $\{P_{\psi_A}, P_{\psi_B}\}=P_{\psi_A}P_{\psi_B} + P_{\psi_B}P_{\psi_A}$, and the belief 'similarity' of both states, λ, is defined in Eq.(6). The prior and posterior belief states, mediated through the Hamiltonian, govern the cognitive process associated with the experimental paradigm. A morphing model therefore requires an adjusted parametrization of both a person's initial belief state and any potential effects of decision-making settings on their final belief state (see Section 7).

5. Belief state hopping dynamics

The quantum-like morphing dynamics allows the cognitive rumination process from social information to evolve –in general– over (finite-dimensional) multi-attribute belief states. Here, the experimental paradigm of Granovskiy et al. (2015) requires shifting a response value over a numerical range (see Section 6). In similar experimental setting, the cognitive process for evidence sampling and valence development prior to responding have been modeled using drift- diffusion models, both with a classical and quantum-like random walk formalism. In that framework not only

[8]This non-matrix-exponential expression allows an analytical insight into the morphing process and provides a faster algorithm for numerical computations.

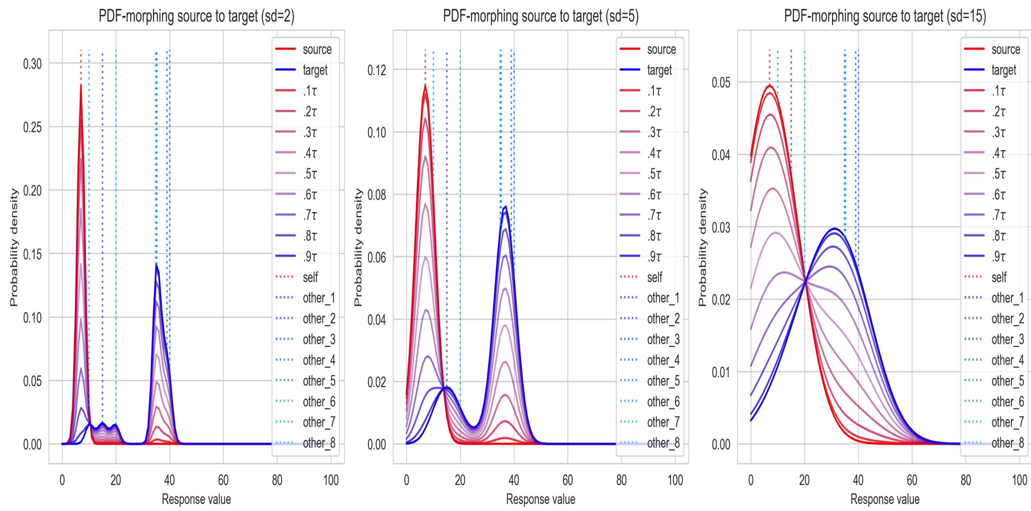

Figure 1: Morphing evolution of a belief probability distribution from source (red) to target (blue). In ten time steps, each of size $\tau/10$, the source distribution evolves into the target distribution as shown by the curves with hue changing from red to blue. Three cases are given for which the uncertainty of the response values is increased in each through larger values of the standard deviations on the probability distributions; SD=2 (left), SD=5 (middle), and SD=15 (right). For these cases of uncertainty, the *final* states show a multi-modal, bi-modal or uni-modal characteristic respectively, while the *source* state remains unimodal and only widens accordingly. Note that this example presents SD-variations of the tested *multi-model* target state for group session 17, student ID 30, question ID 23, round 2; the student's own response value is indicated by the red dotted vertical line, and the eight other response values - the crowd's responses - appear as blue dotted vertical lines.

choice proportion but also response-time can be modeled.

Following Feynman's description of Schrödinger's evolution on a linear crystal lattice, and Bhattacharya and Waymire (1992)'s description of the 1-dimensional Markov drift-dispersion model, a 1-dimensional drift-diffusion model for transitioning over *confidence* levels was implemented in decision models by Diederich (1997); Diederich and Busemeyer (2003); Busemeyer et al. (2006b). For comparison with the morphing approach, we also implement a *hopping* dynamics approach. The corresponding classical dynamics will be developed by Markov hopping for response values accordingly. The quantum-like hopping evolution formally resembles a ladder step-movement on a discretized one-dimensional crystal lattice, instead of a drift-diffusion. Originally Hubbard (1963) solved the lattice systems in which an electron's dynamics is governed by hopping or tunneling to adjacent atoms, and local on-site repulsion. Its adapted one-dimensional discretized form has been applied in e.g., spinfoam dynamics (Feller and Livine, 2017). These models rely on first-neighbor interactions and local potential energies of the discrete components, through the Hamiltonian's action on the state function

$$H\psi = \begin{bmatrix} \ddots & z_{k-1} & 0 \\ z_{k-1}^{\star} & d_k & z_k \\ 0 & z_k^{\star} & \ddots \end{bmatrix} \begin{bmatrix} \vdots \\ r_k e^{i\varphi_k} \\ \vdots \end{bmatrix} \tag{12}$$

where the state components $r_k \in \mathbb{R}$ and $\varphi \in (0, \pi)$ and the $z_k{=}a_k e^{i\vartheta_k}$ are the complex-valued Hamiltonian driver components.[9] The dynamics becomes apparent by splitting the Schrödinger equation $i\partial_t \psi = H\psi$ into its real and complex components:

$$\begin{aligned} \dot{r}_k &= a_{k-1} r_{k-1} \sin(\varphi_{k-1} - \varphi_k - \vartheta_k) + a_k r_{k+1} \sin(\varphi_{k+1} - \varphi_k + \vartheta_k), \\ r_k \dot{\varphi}_k &= -d_k r_k - a_{k-1} r_{k-1} \cos(\varphi_{k-1} - \varphi_k - \vartheta_k) - a_k r_{k+1} \cos(\varphi_{k+1} - \varphi_k + \vartheta_k). \end{aligned}$$

[9]The signed modulus convention allows to identify the phase inversion of reflection off a potential wall through negative r_k.

The drift-diffusion model sets ϑ_k=0, and identifies a_k=${\sigma_k}^2/\Delta^2$ as the diffusion rate and d_k=$k \cdot \mu/\Delta$ as a linear potential (Busemeyer et al., 2006b).[10] The hopping model sets ϑ_k=$\pm\pi/2$, and identifies a_k as the hopping rate. For belief state value-shifting or response 'flexibility', no differentiation of the hopping parameter over the k-range is required, fixing a_k=a, but its variation can be considered when modeling a distinct effect for a nearby (e.g. slow-down) or remote (e.g. speed-up) target (Diederich and Busemeyer, 2003). With the hopping dynamics implemented through parameter a, no additional potential energy term is required to engender change, allowing to set d_k=0,

$$\begin{aligned} \dot{r}_k &= a\left(r_{k+1}\cos(\varphi_{k+1} - \varphi_k) - r_{k-1}\cos(\varphi_{k-1} - \varphi_k)\right) \\ r_k\dot{\varphi}_k &= a\left(r_{k+1}\sin(\varphi_{k+1} - \varphi_k) - r_{k\text{-}1}\sin(\varphi_{k\text{-}1} - \varphi_k)\right) \end{aligned} \tag{472}$$

The change of the belief amplitude r_k is governed by the hopping rate parameter a, and requires a non-zero net of inflowing $(k+1)$ and outflowing $(k-1)$ amplitudes from neighboring compounds weighted by their phases' difference cosine.[11]

For an initial real-valued state vector, the phase evolution equation becomes $\dot{\varphi}_k$=0, and state vectors remain real-valued over time. The hopping dynamics, $\dot{r}_k$=$a(r_{k+1} - r_{k-1})$, shows a wave packet moves k-downward for a>0 and r_k>0, since an amplitude r_k waxes ($\dot{r}_k$>0) in a k-increasing wave front,

[10] the parameter Δ allows to attain the diffusion case over one continuous space dimension when its limit goes to zero.

[11] In comparison, a diffusion model will take the weighted average of neighbor components instead.

while it wanes ($\dot{r}_k$<0) in a k-decreasing wave front. The velocity of the belief state over the k-range is easily derived from the hopping equation, using r_{k+1} - r_{k-1}=(r_{k+1} - r_k) + ($r_k - r_{k-1}$) $\approx 2\delta r_k$ and δk=1, allowing the approximate notation;

$$(r_{k+1} - r_{k-1}) - \frac{\dot{r}_k}{a} = 0 \quad \Rightarrow \quad \left(\frac{\partial}{\partial k} - \frac{1}{2a}\frac{\partial}{\partial t}\right) r_k = 0.$$

Identifying the quantum-like hopping velocity v_k=$2a$, reveals the evolution period towards attaining the target value $\tau_{hop} = \frac{|k_{target}-k_{source}|}{2a}$.

Besides the basic hopping dynamics, a core feature is the dynamics at zero-points of a_k on the k-range: inserted target points k=k_T, or the end points, k=0 and k=100. At the target point k_T, the hopping stops, requiring the velocity coefficient be set to zero, a_{k_T}=0. Then the two neighboring amplitudes above the target follow $\dot{r}_{k_T+1} = ar_{k_T+2}$ and $\dot{r}_{k_T+2} = a(r_{k_T+3}$ - $r_{k_T+1})$, which combine to $\ddot{r}_{k_T+1} + a^2 r_{k_T+1} = a^2 r_{k_T+3}$. The bordering amplitude r_{k_T+1} to the target hence follows a second-order linear nonhomogeneous ODE with constant coefficients, showing r_{k_T+3}-driven oscillatory solutions.[12] With the real-valued amplitude convention, the occurring sign-inversion of r_{k_T+1} corresponds to the phase inversion of the wave reflection on the wall of a potential well, Fig.2.

The hopping dynamics allows continuous change of one's response value towards –or away– of a target value. In the current implementation, it describes the movement of the response value itself, not its confidence

[12] Similarly, on the complementary interval below the target point $\dot{r}_{k_T}$=$-ar_{k_T-1}$ and $\dot{r}_{k_T-1}$=$a(r_{k_T}$ - $r_{k_T-2})$ with $\ddot{r}_{k_T}$ + $a^2 r_{k_T}$=$a^2 r_{k_T-2}$ showing oscillation.

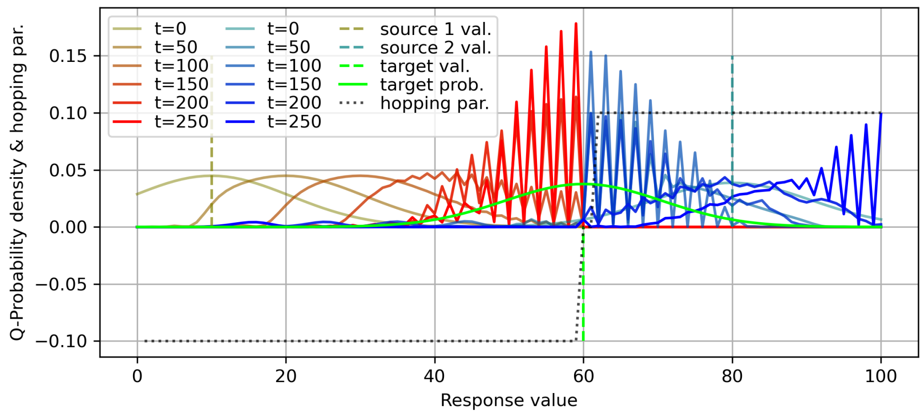

Figure 2: Example of quantum-like hopping dynamics of belief probability masses (SD=15) from two source values, at '10' and '80', from both sides of a target value k_T=60, at five consecutive time stages and velocity parameter a=.1 . Notice the wave-like oscillation pattern when the probability mass nears the target (left and right). For comparison both waves were given the same time range of evolution. Since the left wave originated from a larger k-distance, its travel time to the target value is longer. In that same time range the right wave reached the target, reversed direction and already bounces off the opposite range edge, illustrating the requirement to constrain time to the hopping period.

level. A respondent, for example, who initially chooses an outlier value may afterwards partially concede by moving toward a value closer to the group mean, would intuitively be characterized as *hopping* along the response scale, rather than collapsing directly into a new belief distribution as in morphing. A hopping dynamics is therefore only appropriate in experimental paradigms where numeric or ordinal responses can shift gradually (Likert-scaled tests, estimation tasks).

Also the quantum-like hopping approach provides an adequate dynamics to move a prior belief into a posterior one. In this approach the hopping Hamiltonian will let the initially contrived response value travel towards a specific target value - given the adjusted parametrization in the Hamiltonian.

Markov hopping. The corresponding Markov process is devised to evolve, through classical transition intensity, an individual's belief over their response values while influenced by social information. A similar neighbor-dynamics over response values can be implemented in the Markov intensity matrix (Diederich and Busemeyer, 2003). The hopping evolution in the Markov formalism is hence provided by the intensity K, left-acting on the probability vector Π according to

$$K\Pi = \begin{bmatrix} \ddots & u_{k\text{-}1} & 0 \\ l_{k\text{-}1} & \text{-}u_{k\text{-}1}\text{ - }l_k & u_k \\ 0 & l_k & \ddots \end{bmatrix} \begin{bmatrix} \vdots \\ p_k \\ \vdots \end{bmatrix} \tag{13}$$

with $l_k \geq 0$ and $u_k \geq 0$, and zero within-column sums for total probability conservation:

$$\dot{p}_k = l_{k-1}p_{k-1} - l_k p_k + u_k p_{k+1} - u_{k-1}p_k. \tag{14}$$

Switching off the lower diagonal elements, l_k=0, and denoting $p_{k+1}\text{-}p_k \approx \partial p_k$ and ∂k=1, shows a pulse with (approximate) velocity u_k and k-decreasing over time; $\left(\frac{\partial}{\partial k} \text{ - } \frac{1}{u_k}\frac{\partial}{\partial t}\right) p_k$=0. While switching off the upper diagonal elements, u_k=0, shows a pulse with approximate velocity l_k and k-increasing over time; $\left(\frac{\partial}{\partial k} + \frac{1}{l_k}\frac{\partial}{\partial t}\right) p_k$=0. In particular, the hopping intensity matrix towards a target k_T requires the upper diagonal set to zero for $k < k_\mathrm{T}$ and the lower diagonal set to zero for $k \geq k_\mathrm{T}$.[13] The boundary dynamics in

[13]For probability conservation this requires setting diagonal elements $K_{k_\mathrm{T}k_\mathrm{T}}$=$K_{k_{\mathrm{T}\text{-}1}k_{\mathrm{T}\text{-}1}}$=0, Eq.(13).

the Markov case is known to differ from the oscillatory pattern in q-like dynamics (Busemeyer et al., 2009). Case in point, for a target set at k_T, the target and near-target probabilities satisfy $\dot{p}_{k_\mathrm{T}}=up_{k_\mathrm{T}+1}$, and $\dot{p}_{k_\mathrm{T}\text{-}1}=lp_{k_\mathrm{T}\text{-}2}$. Both probabilities show monotonous increase, feeding on incoming probability mass (respectively from up and down the target value), i.e. the expected pile-up behavior of a hopping Markov process at the boundary, Fig.3.

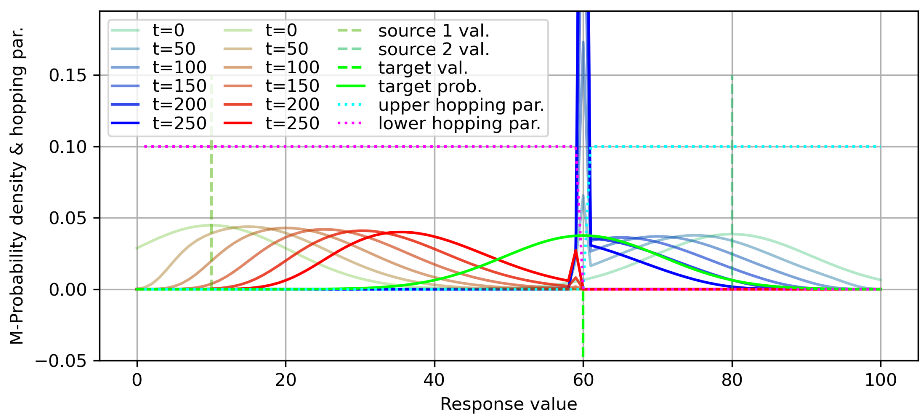

Figure 3: Example of Markov hopping dynamics of belief probability masses from two sources, response values '10' and '80', from both sides of a target value k_T=60, at five consecutive time stages and velocities u=0, l=.1 (left), and u=.1, l=0 (right). The probability masses from both sides accumulate at the target value and evolve into a stationary distribution.

6. Social-influenced decision making: the Granovskiy et al experiment

The belief morphing approach is implemented to model social influence in an experiment setup by Granovskiy et al. (2015) that tested the effect of *crowd-wisdom*, and for which we were provided the data. In the experiment, all the individuals in a group can change their answers to the same question over different rounds. The questions concern some trivia to which the correct answer is a number in the percentage range [0, 100].

In the first round, each participant responds to the question on their own. After the first round, when all responses are registered, each individual gets to see the other participants' responses and now is tasked to respond again to the same question, allowing them to adjust their first response. The responses of the second round are registered and once more the new responses of the other participants are shown. The participant is then asked for a final time to respond to the question allowing for a final adjustment of their answer, after which all the last responses are recorded. Therefore, in the first round, responses are given without any contextual information, while in the second and third rounds, each response may be informed by the group's earlier responses.

As Granovskiy et al. (2015) report, undergraduate students from Indiana University were assigned to 38 groups of variable size from 2 to 10 participants for this experiment in 2008. More precisely, after data cleaning, the provided dataset contains –size times number of groups– 2x7 + 3x4 + 4x6 +5x9 + 6x4 + 7x3 + 8x2 + 9x1 + 10x2 or 185 partitioned student sets of responses to all questions in all rounds. These questions were selected from trivia appearing in the 2008 CIA World Factbook to have true responses with values widely spread between 2% and 99% (Central Intelligence Agency, 2008). Any 'crowd' effect in the dataset hence needs to be understood here as resulting from relatively small groups and concerning mostly nonsalient matters.

Our focus here is not so much on the possibility of the progressive improvement of the responses with respect to the exact solution, but on how individual beliefs can change when exposed to information from others' beliefs. The design of this experiment exactly allows for observing how the participant's beliefs in a group influence one another.

The heuristics to change one's response based on other's responses are various. While aiming for *conformity* to avoid discrepancy between an individual and their group seems inherent (Cialdini and Goldstein, 2004), the 'unemotionally laden nature' of the trivia questions suggests that the context is not a valid underlying driver to conform (Granovskiy et al., 2015). In the given task, the social distribution of responses imparts an informative influence. From the response changes enacted by the participants over the subsequent rounds, the study of Granovskiy et al. (2015) observes that group average performance to close in on the real value improves with group size, supporting the wisdom of crowds hypothesis. Depending on the pointer's middle position on the response slider at start, individuals may show a systematic bias toward 50%; overestimating values below 50% and underestimating values above 50% . This bias follows a linear relationship:

$$b(v(q)) \quad = \quad 0.45v(q) + 26, \tag{15}$$

where $v(q)$ is the correct answer to question q. The authors note that 68.9% of participants made no changes to their guesses between rounds. They conclude that social information provides a small but significant improvement to group performance. Individuals in groups improved over rounds, while solo individuals did not. The strongest effect was convergence to the group mean (25.2% reduction in distance from Round 1 to 2). Group 'polarization' also occurred - estimates became more extreme over rounds, counteracting the initial bias toward 50%. Outlier behavior was the main driver for improvement of group accuracy, by their moving toward the group mean.

7. Cognitive influences in group decision making

In Granovskiy et al. (2015)'s social-information experiment, each next decision of a participant is influenced by the contextual information derived from other participant responses. A variety of cognitive processes can underlie the reasoning which goes into each individual's subsequent responses. Unlike a Bayesian updating process, each individual respondent does not need to accept the information from the group as *case evidence*. Depending on their proper knowledge and strategy, each respondent evaluates the information of the group's responses differently. For instance, when a respondent is certain about their response, they should stay with their choice in the next stages, but conformity bias or a degree of socially desirable responding confirmation bias can sway their choice. On the other hand, when a respondent is to some degree uncertain about their response, they may want to 'improve' their choice in the next stage by interpreting the incoming information from other participants. When the distribution of incoming choices seems to be directly informative - e.g., the choices concentrated about some value - then in the next stage the respondent may shift their response towards this value. More complicated processes may occur when the response distribution seems multi-modal, shows disparately scattered responses, or with various apparent outliers.

In the previous section, belief state morphing was shown to model the dynamics for a controlled transformation between any two given states. Some heuristic strategies to improve a respondent's response are now devised in target states.

In the first round, respondent-i's belief state for a response to a particular question, with possible response values in $[0, 100]$, is set to a re-normalized Gaussian about response R_{1i} as its mode, the most probable value of response. A specified standard deviation SD_{1i} expresses the inherent uncertainty of the respondent concerning their own choice in the first round

$$\psi_i(v) = \mathscr{E}_i(v)/\mathscr{N}_i, \tag{16}$$
$$\mathscr{E}_i(v) = e^{-\frac{(v-R_{1i})^2}{2\sigma^2}}, \quad \mathscr{N}_i = \left(\mathscr{E}_i^\dagger \mathscr{E}_i\right)^{1/2}, \quad \sigma = \mathrm{SD}_{1i},$$

with $v \in [0, 100]$. In essence, the belief state allocates probability mass over the range of choice according to their knowledge, intuition or bias of the respondent. The individual responses of the group on the same question provides 'prior' information, which can influence the respondent's next response to this same question. This information can be interpreted in various ways; e.g. aggregated to a other-group's median of answers, or perceiving a distribution composed of all other-group's answers and assumed uncertainty.

7.1. Belief target design

A set of quantum-like models –morphing or hopping– are tested which each have a different underlying cognitive heuristic, expressed through specific target belief state. Subject to the experiment's observations, the most effective cognitive heuristic model could then be distinguished. The participant's task in Granovskiy et al. (2015) experiment is to give their best possible response to the questions, and the target belief state of the heuristic will hence include information derived from the other responses. Various crowd-wisdom aggregation methods can be derived from the work of Sherif et al. (1958); Lyon and Pacuit (2013); Moussaïd et al. (2013); Flache et al. (2017), which in our study are focused according to either of the following principles:

- The target belief is the ***multi-modal composition*** of other's response distributions. This heuristic does not process the information of the response distribution, other than compounding it unchanged into a multi-modal distribution. Cognitively, this target belief state adds the supplementary information from the imagined possible variability of the other's answers – the SD variable, Eq.(16). Summing the other's distributions can give rise both to dense concentrations and more sparse comb-like distributions. When the distribution of the group's responses as such is acquired as information, the target morph state is built as the unbiased sum of all individual response peaks $\mathscr{E}_j$, Eq.(16),

$$\begin{aligned} \psi_{\text{multi}_i}(v) &= \textstyle\sum_{j\neq i} \mathscr{E}_j(v)/\mathscr{N}, \\ \mathscr{N} &= \left(\textstyle\sum_{j\neq i} \mathscr{E}_j^\dagger \sum_{k\neq i} \mathscr{E}_k\right)^{1/2}, \end{aligned} \tag{17}$$

  where for model parsimony, the uncertainty σ on each respondent component is subsumed with the same value SD.

- The target belief is the ***median*** of other responses. This heuristic understands that most responses are guesses about the correct answer and subsume a normal dispersion of responses about the correct value. This heuristic may fail when the apparent PDF is multi-modal, e.g. when the crowd is polarized around two or more values. In that case, nesting the target value in the middle of the peer's choices would miss sub-group information but appease polarization or dissonance. Targeting the *mean* value instead would be prone to absorbing the effect of far outliers. When the posterior information is aggregated to the median value of the group's responses and the spread of the answers is understood as an informative measure of uncertainty, the target morph state is itself built along the single mode Gaussian approach, Eq.(16),

$$\psi_{\mathrm{med}_i}(v) = \mathscr{E}_i(v)/\mathscr{N}_i, \qquad (18)$$
$$\mathscr{E}_i(v) = e^{-\frac{(v-\overline{R_1}_{\neq i})^2}{2\sigma_i^2}}, \quad \sigma_i = \mathrm{SD}_t,$$

where $\overline{R_1}_{\neq i}$ denotes, for participant i, the median of other previous responses (from the first round). While in principal, respondent i could formally derive a value for the standard deviation of the other's responses, our approach sets the σ_i to an intuited fixed value SD_t in the target state. This projected uncertainty is varied and its effect on model performance is monitored.

- The target is the ***maximal concentration*** zone of other responses. A more dense concentration in the response distribution may appear as a focus region with less uncertainty about the possible response. It could quantitatively reflect the informed support for a response in a particular zone. This heuristic will be more straightforward to apply when the group size is larger. Moreover, the range of this perceived concentration zone may vary with group size, and guided by cluster details respondents may aim asymmetrically from the middle of this concentration zone. An algorithm, using a sliding window of size w, searched the maximum density zone on the density function of the multi-modal state, Eq.(17).

$$\psi_{\max_i}(v) = \mathscr{E}_i(v)/\mathscr{N}_i, \tag{19}$$
$$\mathscr{E}_i(v) = e^{-\frac{(v-x_{max})^2}{2\sigma_i^2}}, \quad x_{max} = \frac{w}{2} + \arg\max_x \int_x^{x+w} |\psi_{\text{multi}_i}(x')|^2 dx'$$

This size of the sliding window was taken fixed, and in correspondence to most of the change of response between rounds (see Fig.B.6), figuring as a measure of relevant response difference. The algorithm finds the position of the window over the distribution range for which the composite trapezoidal rule of integration is maximal, and the median of that window resulted in the target value. Also here, the uncertainty σ_i is fixed to SD_t in the target state.

Other heuristics that may be less common could be put forward but will not be implemented for the conciseness of our presentation. For instance, in an acquainted group, the target belief of a participant could follow a **preferred-other**'s responses. This heuristic is only possible if the responses of all participants are recognizably id-tagged. In another more conservative approach, a respondent will base their target belief on those responses that stand most similar, and may then resort to an **n-nearest** averaging for their next response. Especially in more scattered response distributions, the responses of those closer to their own response may receive more weight when deciding their next response. The three discussed target variations above are hence adopted in our model; the 'multi' version of the model aims for the composition of other's belief state target, and the 'median' version aims for the truncated gaussian about the median of other's responses, the 'max' version aims for a truncated gaussian about the middle of a perceived maximum density of the other's responses. Since respondents may well switch choice strategies and related target beliefs over the experiment, an individual response-based analysis for model-switching will be done. The morphing dynamical approach with source-target formulation can be applied in various ways, in particular according to 'idealized' targets or parametrized targets. Targets can be expressed according to various 'ideals', or heuristics, and competing their performance with respect to the observations reveals what groups adhere to what ideal target states. On the other hand, when a target is parametrized rather than a fixed ideal, the model does not presuppose competing solutions. The fitted target parameters then summarize which aspects of the social information best account for observations, and thereby serve as a diagnostic of a possible underlying 'ideal' or heuristic that guides belief change. In general, in morphing dynamics the parameters in the target state need to be identified by the experimental paradigm of the problem at hand, and how its Hilbert space was organized (see Appendix C). In our current implementation with the

Granovskiy et al. (2015) paradigm, the targets present a mix of heuristics and parametrisation, inferring their parameter values from observations.

In the studied experimental setting (see Section 6), respondents move a slider from default value '50' to a response value in the range of '0' to '100'. Each individual responds according to their current belief state, and during measurement will collapse the probabilistic state for an answer to a stated actual response value. With the complex information input from possibly multi-modal target states, an alternative method of threshold variation to obtain the optimal response is not applicable here (see e.g. Khodadadi et al. (2014)). Based on a principle of comparative evidence, the potential **response value** with the highest probability, at the optimal evolution time, becomes the response value: *i.e.* the argmax of the belief probability distribution of the final morphed state. Lacking individual personal features of responders in the experimental paradigm of Granovskiy et al. (2015), all model predictions could then deterministically realize the argmax of the designed target outcome. To capture possible *inter-respondent variability*, we introduce random sampling of the surrounding of the argmax of a respondent's belief probability density. Ultimately, this temperature-dependent Gumbel sampling will set the final response of an individual (Maddison et al., 2014). The Gumbel sampling produces responder-diversity by simulating latent variables that generate observable individual differences (see Appendix D). A temperature parameter allows the model to control the sampling neighbourhood about the argmax, with high temperatures causing low variation. This approach satisfies the probabilistic nature of the cognitive state but still favors random responses near the maximum probability response.

8. Models, assessment and performance comparison

The performance of the quantum and classical models with three different targets, 'multi', 'median', and 'max' are tested on the trivia data set.

All models make predictions for each of the 38 groups, for each of the 36 questions, for each student in the group (variable, 2 to 10), for each informed round (2 informed rounds, the first round is not informed), and produce a residual error which needs to be minimized.[14]

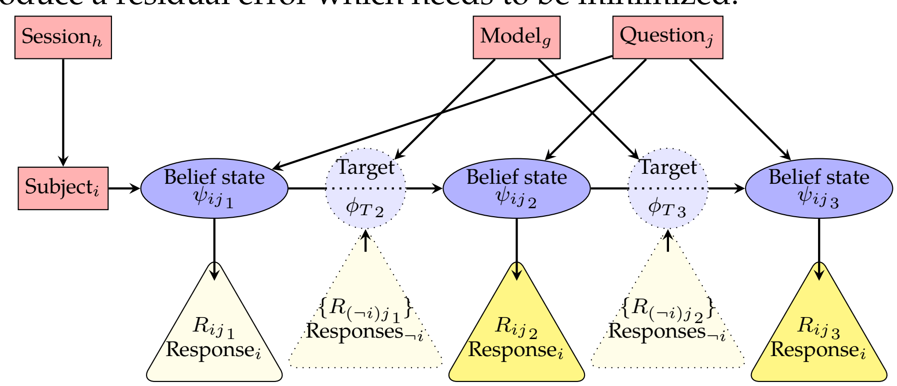

A priori, the parameter space for error-optimization has two parameters at the model level, $T \in \{.2, 2, 20, 200, 2000\}$ and SD $\in \{5, 10, 15, 20, 25\}$ (range based on observed bias-variation, Eq.(15).) and, one parameter $t_{\text{frac}} \in \{0, .., 100\}$ at the observation level.

The effect of temperature on the outcome generation by Gumbel sampling is significant, see Appendix D : the trial-and-error exploration vs model-

[14] The data cleaning was needed in two groups: in Group 21, student with ID 31 stops playing from question rank 22 in round 1, then stops fully, and in Group 27, student with ID 33 stops playing from question rank 24 in round 3, then stops fully. In order not to lose valid data samples from the other students, it was decided to impute the missing values with averages of the other's responses.

predictivity needs to be balanced. The next subsection explains its mitigation by limiting the sample temperature range.

8.1. Individual response variation and Gumbel sampling temperature

The interaction between the distribution's uncertainty and temperature may appear counter-intuitive. With broader belief distributions (higher standard deviations), the large multiplication factor from low temperatures can cause many sampled values –out of the model's intended scope– to compete with the true predicted maximum. This could create an abundant trial-and-error effect, unsupported by the underlying model. A recommended temperature range needs to be explored which is not too low to avoid unwarranted sample variation, and not too high to maintain typical human response variability w.r.t uncertainty. With lower temperatures consistently producing better average MAE scores (Mean Absolute Error), Fig.D.9, the increased exploration could be helping the model escape local optima or better capture the underlying data structure.[15] The anti-intuitive effect of the temperature in the Gumbel sampling is due to the larger standard deviations that are chosen on the belief states. If the belief distribution is chosen more spiked (e.g., SD=2), then choosing a low temperature would make the perturbed distribution more spiked. Also the subsumed width of the belief distributions needs to be kept in range: lower bounds of SD=5 tend to generate computational log 0 errors, while SD>25 is too indefinite w.r.t. decision precision cases.

Taking into consideration the effect of the Gumbel temperature on the

[15] An individualized temperature could be considered to further define each respondent, but the parameters space would increase and require compute accordingly.

response sampling, its value has been fixed to 20 for a balanced exploration-exploitation ratio.

8.2. *Statistical evaluation*

In effect, each of the 9x5 model-SD variants contain one free parameter type, the evolution time t_{frac}. This parameter is estimated independently for each question, resulting in 72 fitted parameter values per student (one per question).

Model level. To analyze the model complexity and performance of each model, the Bayesian Information Criterion (BIC) for each of the 45 models was calculated. The standard formulation of BIC is used; $\text{BIC} = n\log(\text{RSS}/n)+k\log(n)$. Where RSS is the residual sum of squares, $n = 13320$ is the number of observations in the Granovskiy et al. (2015) dataset, and the complexity penalty term with k=$2 \cdot 36$ uses the same number of free parameters in each of the 45 compared models.

Model	SD=5	SD=10	SD=15	SD=20	SD=25
Q-multi-morph	198421 (3.600)	194261 (3.079)	190634 (2.687)	187141 (2.357)	184265 (2.116)
Q-median-morph	199209 (3.708)	195313 (3.203)	191474 (2.773)	187767 (2.413)	184683 (2.149)
Q-max-morph	199247 (3.713)	195294 (3.201)	191334 (2.759)	187634 (2.401)	184393 (2.126)
Q-multi-hop	204772 (4.568)	203171 (4.302)	201816 (4.089)	200379 (3.874)	199405 (3.735)
Q-median-hop	204810 (4.575)	203272 (4.318)	201611 (4.057)	200358 (3.871)	199693 (3.776)
Q-max-hop	204815 (4.576)	203220 (4.310)	201680 (4.068)	200355 (3.871)	199422 (3.737)
M-multi-hop	192174 (2.847)	192077 (2.837)	192793 (2.914)	194055 (3.055)	195446 (3.219)
M-median-hop	192208 (2.851)	192079 (2.837)	192682 (2.902)	193807 (3.027)	195683 (3.248)
M-max-hop	192216 (2.852)	192043 (2.833)	192760 (2.910)	193953 (3.044)	195713 (3.252)

Table 1: BIC (RMSE) values for optimized models over fixed SD values for the morph parameter t_{frac}. For all 45 models, the number of free parameters per student is 72, the total number of parameters is 13320, and the total number of observations is 13320. The Gumbel temperature T=20.

The best-BIC performing model is the Q-multi-morph SD=25 model with the lowest BIC value of 184265 and an average RMSE of 2.116.

To assess the significance of the morphing parameter across the full cohort, a one-sample t-test is performed on the distribution of fitted parameter values across all 13,320 observations (185 students × 72 questions). For each model, the one-tailed t-test analysis reports p-values testing the hypothesis that the morph parameter is greater than zero ($H_1 : t_{\text{frac}} > 0$), given its range [0,1]. The analysis, Table 2, demonstrates that dynamical evolution parameter t_{frac} is statistically significant in all of the models (α=0.05). In the best BIC-performing model (Q-multi-morph, SD=25, T=20), the morphing parameter showed a mean value of 0.133 (Std err=.001, N=13320, 95% CI: 0.130-0.135, t(13319)=90.826, p<0.001), indicating a reliably non-zero value across observations, Table 2.

Table 2: Estimated morph parameter statistics (T=20).

Model	SD	Par	N_Obs	Mean	Std_Err	t_stat	p_val	CI L_95	CI U_95
M-max-hop	5	t-frac	13320	0.067	0.145	0.001	0.000	0.065	0.070
M-max-hop	10	t-frac	13320	0.057	0.109	0.001	0.000	0.056	0.059
M-max-hop	15	t-frac	13320	0.044	0.080	0.001	0.000	0.043	0.046
M-max-hop	20	t-frac	13320	0.035	0.062	0.001	0.000	0.034	0.036
M-max-hop	25	t-frac	13320	0.028	0.047	0.000	0.000	0.027	0.028
M-median-hop	5	t-frac	13320	0.068	0.146	0.001	0.000	0.065	0.070
M-median-hop	10	t-frac	13320	0.057	0.108	0.001	0.000	0.055	0.059
M-median-hop	15	t-frac	13320	0.044	0.081	0.001	0.000	0.043	0.045
M-median-hop	20	t-frac	13320	0.034	0.060	0.001	0.000	0.033	0.035
M-median-hop	25	t-frac	13320	0.027	0.046	0.000	0.000	0.026	0.028
M-multi-hop	5	t-frac	13320	0.068	0.146	0.001	0.000	0.065	0.070
M-multi-hop	10	t-frac	13320	0.057	0.108	0.001	0.000	0.055	0.059
M-multi-hop	15	t-frac	13320	0.044	0.081	0.001	0.000	0.043	0.046
M-multi-hop	20	t-frac	13320	0.034	0.060	0.001	0.000	0.033	0.035
M-multi-hop	25	t-frac	13320	0.027	0.047	0.000	0.000	0.027	0.028
Q-max-hop	5	t-frac	13320	0.063	0.163	0.001	0.000	0.060	0.066
Q-max-hop	10	t-frac	13320	0.070	0.149	0.001	0.000	0.067	0.072
Q-max-hop	15	t-frac	13320	0.076	0.146	0.001	0.000	0.074	0.079
Q-max-hop	20	t-frac	13320	0.085	0.153	0.001	0.000	0.082	0.087
Q-max-hop	25	t-frac	13320	0.094	0.164	0.001	0.000	0.091	0.097
Q-max-morph	5	t-frac	13320	0.084	0.186	0.002	0.000	0.081	0.087
Q-max-morph	10	t-frac	13320	0.099	0.179	0.002	0.000	0.096	0.102
Q-max-morph	15	t-frac	13320	0.110	0.171	0.001	0.000	0.107	0.113
Q-max-morph	20	t-frac	13320	0.121	0.166	0.001	0.000	0.118	0.124
Q-max-morph	25	t-frac	13320	0.131	0.166	0.001	0.000	0.128	0.134
Q-median-hop	5	t-frac	13320	0.062	0.162	0.001	0.000	0.060	0.065
Q-median-hop	10	t-frac	13320	0.070	0.149	0.001	0.000	0.068	0.073
Q-median-hop	15	t-frac	13320	0.076	0.146	0.001	0.000	0.073	0.078
Q-median-hop	20	t-frac	13320	0.085	0.154	0.001	0.000	0.082	0.087
Q-median-hop	25	t-frac	13320	0.094	0.166	0.001	0.000	0.091	0.097
Q-median-morph	5	t-frac	13320	0.084	0.188	0.002	0.000	0.081	0.088
Q-median-morph	10	t-frac	13320	0.100	0.178	0.002	0.000	0.097	0.103
Q-median-morph	15	t-frac	13320	0.110	0.169	0.001	0.000	0.107	0.113
Q-median-morph	20	t-frac	13320	0.120	0.167	0.001	0.000	0.117	0.123
Q-median-morph	25	t-frac	13320	0.133	0.165	0.001	0.000	0.130	0.136
Q-multi-hop	5	t-frac	13320	0.062	0.161	0.001	0.000	0.059	0.064
Q-multi-hop	10	t-frac	13320	0.070	0.151	0.001	0.000	0.068	0.073
Q-multi-hop	15	t-frac	13320	0.076	0.146	0.001	0.000	0.074	0.079
Q-multi-hop	20	t-frac	13320	0.084	0.153	0.001	0.000	0.081	0.087
Q-multi-hop	25	t-frac	13320	0.094	0.165	0.001	0.000	0.091	0.097
Q-multi-morph	5	t-frac	13320	0.104	0.221	0.002	0.000	0.100	0.107
Q-multi-morph	10	t-frac	13320	0.113	0.205	0.002	0.000	0.109	0.116
Q-multi-morph	15	t-frac	13320	0.119	0.188	0.002	0.000	0.116	0.122
Q-multi-morph	20	t-frac	13320	0.126	0.177	0.002	0.000	0.123	0.129
Q-multi-morph	25	t-frac	13320	0.133	0.168	0.001	0.000	0.130	0.135

Individual level. It is plausible that individual respondents may change their strategies during the task depending on the question or the appearance of the revealed response distribution. To capture this type of individual strategy variability, a statistical analysis of the best RMSE across all models is conducted.

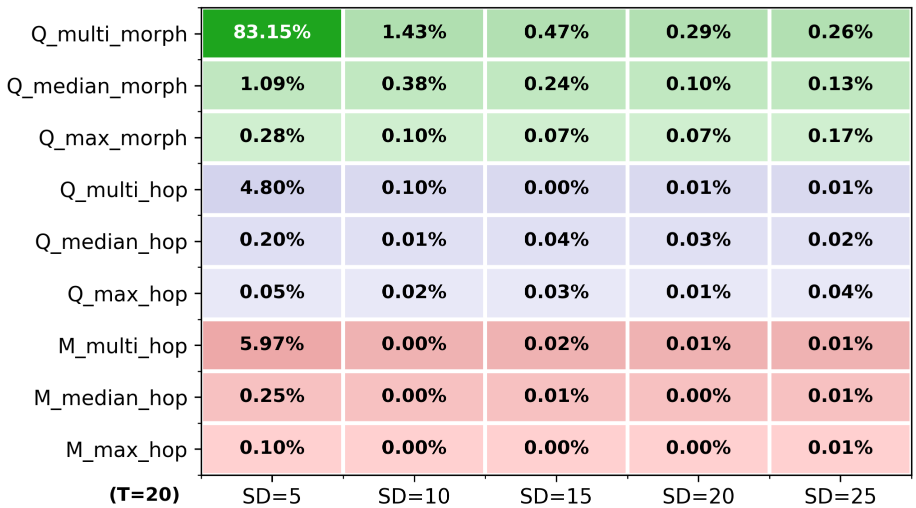

Figure 4: The individual RMSE win rate heatmap over all model-SD combinations (T=20). The frequency-based best model is Q-multi-morph with SD=5. In hopping dynamics the Markov-based M-multi-hop with SD=5 outperforms the quantum-based Q-multi-hop model

Each model variant contains one parameter type, the fractional morphing time $t_{\mathrm{frac.}}$. This parameter is estimated independently for each question by minimizing the RMSE between observed and predicted responses for each model. For each student answering twice the 36 questions in informed context, this results in 72 best fitted parameter values per student from 45 models. Effectively, this approach yields a saturated model with zero degrees of freedom at the individual level.[16] The analysis of the counts of the best model at the individual observation level, Fig.4, shows Q-multi-morph with SD=5 to perform best in most of the observed cases: it wins 95.89% of individual observations. This outcome differs from the best model based on the average RMSE metric, a phenomenon related to Simpson's Paradox. The individual level analysis reveals the Q-multi-morph with SD=5 wins the most individual observations, the aggregate level analysis showed the Q-multi-morph with SD=25 has the lowest BIC, or overall average RMSE. This discrepancy happens because Q-multi-morph with SD=5 performs best on typical cases but catastrophically fails on outlier cases, which inflate the overall average RMSE. The Q-multi-morph with SD=25 loses most individual comparisons but better handles outlier cases keeping the overall average RMSE low.

The quantum multi-morph model with SD=25 achieves the lowest average RMSE, making it the preferred model under maximum likelihood estimation for minimizing overall prediction error. However, SD=5 produces the best predictions in 95.89% of individual cases, demonstrating superior typical-case performance despite occasional catastrophic failures. This reveals a trade-off between global optimality (best average) and local optimality (best in most cases), where the quadratic penalty in MLE heavily weights the rare but severe failures of the SD=5 model version.

Finally, the optimal parameter by an individual student for a specific question characterizes their disposition with respect to social information on

[16]Note that all 36 questions in the Granovskiy et al. (2015) experiment are *unrelated*, therefore a model's performance on a training subset cannot generalize to a holdout subset.

that occasion in the experiment. For each individual student their optimal parameters (one per question) can be plotted as a density distribution, e.g. in Fig.5. From the comparison of these parameter violin distributions of each group member in a given session of the experiment the tendency of an individual's *flexibility* can be observed.[17] Since, in the Granovskiy et al. (2015) experiment the participants readjusted relatively few times their response, the distributions are concentrated towards zero, and more so in the third round (right-half of the violin distribution) in comparison the second round (left-half of the violin distribution). Comparison of the distributions among models, shows which model engaged more with the flexibility property from the elongation of the distributions.

9. Discussion and conclusion

Our study introduces a novel quantum-like belief morphing framework, based on the Brassard-Høyer-Grover amplification formalism, to model social influence in multi-agent decision-making contexts. This innovative use of the algorithm lets a subject's prior belief evolve into a posterior belief in proportion to a subject's valence or utility for a *target*-belief.

Here, for Granovskiy et al. (2015)'s experiment, the target belief was set to aggregate –to variable extent– the information embedded in a group's responses. The belief morphing dynamic can effectively cover decision-making settings in which multiple respondents interact by iteratively stating their judgments and contextual information, processing the information,

[17]The *flexibility* of a participant is their proneness to change their choices over different rounds (Granovskiy et al., 2015).

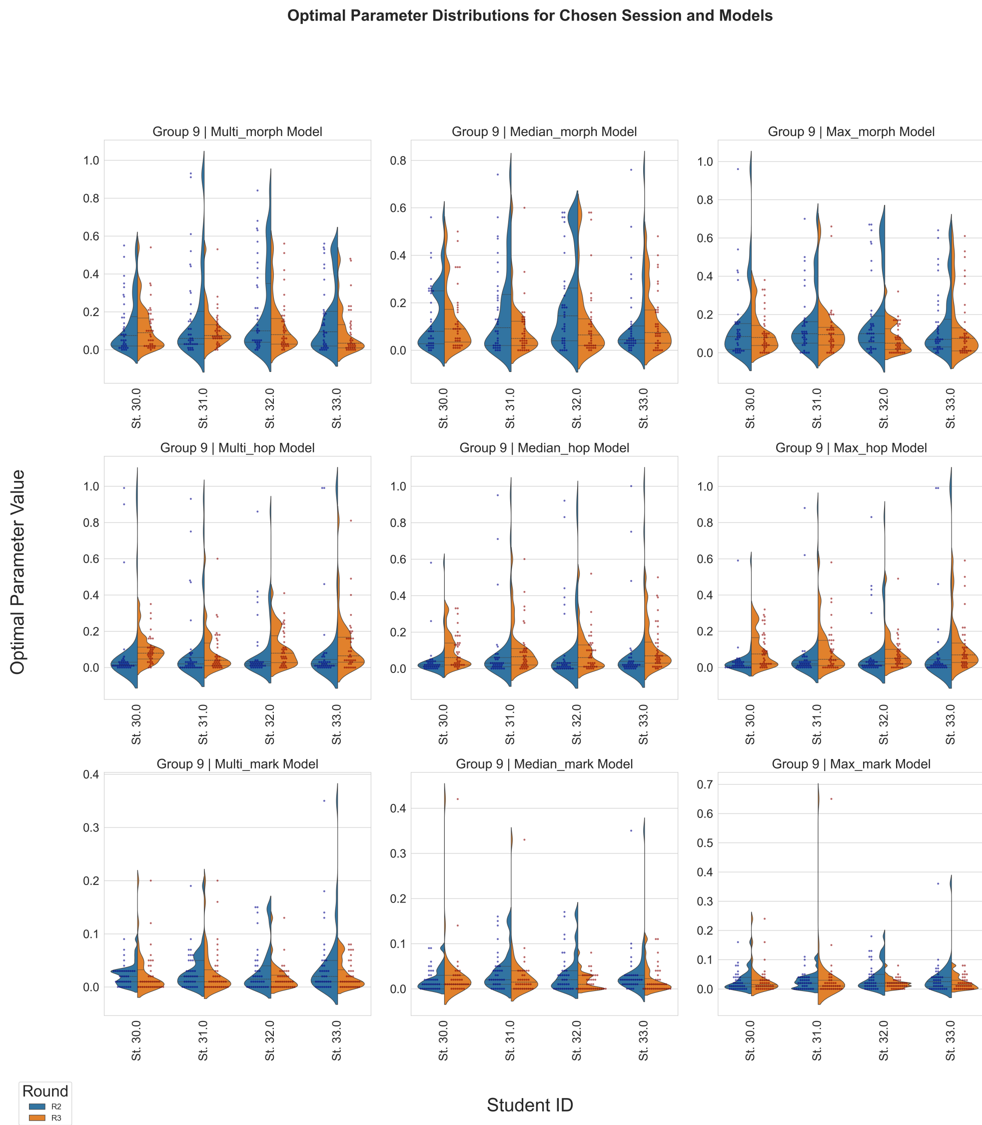

Figure 5: Individual student's optimal t_{frac} parameter distribution over question, in group 9, gathering 4 members, for all nine models Q-morphing (top), Q-hopping (middle), Markov-hopping (bottom), and in columns the target type 'multi' (left), 'median' (center), and 'max' (right). The left half violin (blue) shows the second round optimal parameter distributions for all question, while the right half violin (orange) shows the third round parameter distribution. (T=20, SD=25).

and adapting their judgments in subsequent decisions. In our application to the change of an individual's belief in the crowd-wisdom experiment, the quantum-like morphing model (Q-multi-morph, SD=25) achieved BIC=184265 compared to the best Markov hopping model (M-multi-hop, SD=10) with BIC=192077, Table 1. This represents a substantial improvement in capturing belief dynamics in the social influence paradigm. The better performance of the quantum-like morphing evolution occurred both at the model level (BIC) and at the individual observation level (win rate), but with different intrinsic belief uncertainty (SD=25 vs 5). This effective Simpson's Paradox –the discrepancy between aggregate-level and individual-level model performance– should be taken into account when selecting a model for practical applications. All models showed the evolution parameter t_{frac} was significantly greater than zero ($p<0.001$), confirming that belief change occurred, with the quantum-like morphing (SD=25) providing the best mode of change (effect size: t_{frac}=0.133). The violin distribution plots of the change parameter, Fig.5, revealed substantial heterogeneity in response flexibility, with most participants showing conservative adjustment (concentrated near zero).

In this experiment's crowd-wisdom paradigm, the better performance of the quantum-like morphing model stems from its possibility to formulate detailed *target* belief states. In the application, multi-modal, median, and maximum-density belief states were developed as possible targets. The morphing formalism also allows *interference* effects to shape outcome belief states, but these are expected to become more apparent in other experimental paradigms, for example those involving the disjunction effect.

The ability to devise potential target states is a core feature of the belief morphing approach: competing belief targets can be implemented depending on whether a subject yields to or goes against contextual or group information. Fitting the parameters of competing belief states and comparing their respective model performance enables to reveal tendencies in the underlying cognitive processes. For complex targets, this can be technically done by implementing a tree-structured target state. Dedicated target states, on the nodes of the tree-graph, can each be evolved to by setting to 1 the evolution parameters for the focus branch and quenching the other branches (Appendix C).

The morphing formalism further provides a clear argument for the understanding of the temporal evolution parameter in quantum-like Hamiltonian dynamics. In the morphing approach, the temporal evolution is intrinsically limited. The morphing formalism provides an expression for the period τ in which a source belief has fully morphed into the target belief. Because of this unambiguous limit to temporal evolution, the morphing approach can avoid the characteristic, but cognitively spurious, *periodic* evolution in quantum-like Hamiltonian dynamics. We noted that this issue in the general Hamiltonian approach can be resolved by considering its periodicity, based on the energy spectral decomposition, Eq.(4). In the morphing approach, on the contrary, that period is simply interpreted as the 'time' to reach the target belief, Eq.(10), and allows the best-fitting temporal fraction toward a target belief to be interpreted as a measure of that target's *utility* and as an index of adaptation or flexibility for each respondent.

The quantum-like morphing approach comes with its limitations. At present, it is not developed to cover time-dependent outcomes. The *hopping* dynamical models –quantum-like and Markovian— by contrast include a speed-of-belief-change parameter and could address response-time outcomes. Also, the fixed Gumbel temperature parameter (T=20), the overall adopted perceived uncertainty SD in source and target states, and the uniformly adopted model to fit the *full* cohort, implicitly assume that respondents share, and do not switch, heuristics within the experimental session. While these assumptions served to compare models, these factors should be varied to assess individual respondents. The individual-level statistical analysis of each model's *win rate*, shows that respondents will change response models, Fig.4. The Gumbel temperature, fixing the balance of exploration and exploitation, may also reflect a characteristic interpersonal difference. These issues should be addressed when furthering the morphing approach in different applications.

Finally, the clear interpretational aspect and the formally simple Hamiltonian construction position the quantum-like morphing approach well for future work: revisiting previous experimental paradigms (e.g., the disjunction and conjunction effects, order effects, contextuality, episodic memory recall), expanding it to new paradigmssuch as the evolution of beliefs in social networks, and developing the formalism further to cover time-related experimental paradigms, for example response-time experiments.

Acknowledgments

The dataset used in this study was kindly made available to us by Prof. Robert Goldstone of Indiana University, and was previously developed and analysed in Granovskiy et al. (2015). Stephane Hess and Thomas Hancock acknowledge support from the European Research Council through advanced Grant 101020940-SYNERGY

References

Aerts, D. (2009). Quantum structure in cognition. *Journal of Mathematical Psychology*, 53:314–348. *Cited on page 14*

Aerts, D. and Aerts, S. (1995). Applications of quantum statistics in psychological studies of decision processes. *Foundations of Science*, 1(1):85–97. *Cited on page 9*

Aerts, D., Broekaert, J., Gabora, L., and Sozzo, S. (2016). Editorial: Quantum structures in cognitive and social science. *Frontiers in Psychology*, Volume 7 - 2016. *Cited on page 5*

Aerts, D., Broekaert, J., and Smets, S. (1999). The liar-paradox in a quantum mechanical perspective. *Foundations of Science*, 4:115–132. *3 citations, pages 7, 10, and 20*

Aerts, D. and Gabora, L. (2005). A theory of concepts and their combinations i. *Kybernetes*, 34(1/2):167–191. *Cited on page 9*

Allais, M. (1953). Le comportement de l'homme rationnel devant le risque: Critique des postulats et axiomes de l'ecole américaine. *Econometrica*, 21:503–46. *Cited on page 3*

Asano, M., Ohya, M., Tanaka, Y., Khrennikov, A., and Basieva, I. (2011a). On application of gorini-kossakowski-sudarshan-lindblad equation in cognitive psychology. *Open Systems & Information Dynamics*, 18(01):55–69. *Cited on page 10*

Asano, M., Ohya, M., Tanaka, Y., Khrennikov, A., and Basieva, I. (2011b). On application of gorini kossakowski sudarshan lindblad equation in cognitive psychology. *Open Systems and Information Dynamics*, 18:55–69. *Cited on page 10*

Atmanspacher, H., Filk, T., and Römer, H. (2004). Quantum zeno features of bistable perception. *Biological Cybernetics*, 90(1):33–40. *2 citations, pages 10 and 20*

Bagarello, F. (2019). *Quantum Concepts in the Social, Ecological and Biological Sciences*. Cambridge University Press. *2 citations, pages 5 and 10*

Basieva, I., Pothos, E., Trueblood, J., Khrennikov, A., and Busemeyer, J. (2017). Quantum probability updating from zero priors (by-passing cromwell's rule). *Journal of Mathematical Psychology*, 77:58–69. *Cited on page 20*

Beuria, J., Chaurasiya, M., and Behera, L. (2025). Collective motion from quantum-inspired dynamics in visual perception. *Proceedings of the Royal Society A: Mathematical, Physical and Engineering Sciences*, 481(2321):20250489. *Cited on page 12*

Bhattacharya, R. N. and Waymire, E. C. (1992). *Stochastic processes with applications*. John Wiley & Sons (SEA) Pte. Ltd. *Cited on page 22*

Bocchieri, P. and Loinger, A. (1957). Quantum recurrence theorem. *Phys. Rev.*, 107:337–338. *Cited on page 7*

Brassard, G. and Høyer, P. (1997). An exact quantum polynomial-time algorithm for simon's problem. *Proceedings of the Fifth Israeli Symposium on Theory of Computing and Systems*, pages 12–23. *3 citations, pages 6, 12, and 16*

Brody, D. C. (2023). Quantum formalism for the dynamics of cognitive psychology. *Scientific Reports*, 13(1):16104. *Cited on page 10*

Broekaert, J., Aerts, D., and D'Hooghe, B. (2006). The generalised liar paradox: a quantum model and interpretation. *Foundations of Science*, 11:399–418. *3 citations, pages 7, 10, and 20*

Broekaert, J. and Busemeyer, J. (2017). A hamiltonian driven quantum like model for over-distribution in episodic memory recollection. *Frontiers in Physics*, 5:23. *3 citations, pages 7, 10, and 20*

Broekaert, J., Busemeyer, J., and Pothos, E. (2020). The disjunction effect in two-stage simulated gambles. an experimental study and comparison of a heuristic logistic, markov and quantum-like model. *Cognitive Psychology*, 117:101262. *3 citations, pages 7, 10, and 20*

Broekaert, J. B. and Busemeyer, J. R. (2019). Episodic source memory over distribution by quantum-like dynamics – a model exploration. In Coecke, B. and Lambert-Mogiliansky, A., editors, *Quantum Interaction*, pages 63–75, Cham. Springer International Publishing. *2 citations, pages 10 and 20*

Busemeyer, J. and Bruza, P. (2012). *Quantum models of cognition and decision*. Cambridge, UK: Cambridge University Press. *5 citations, pages 4, 6, 9, 11, and 13*

Busemeyer, J., Matthew, M., and Wang, Z. (2006a). Quantum game theory explanation of disjunction effects. *In R. Sun & N. Miyake (Eds.), Proceedings of the 28th annual conference of the cognitive science society, Mahwah, NJ: Erlbaum.*, page 131–135. *Cited on page 9*

Busemeyer, J., Wang, Z., and Lambert-Mogiliansky, A. (2009). Empirical comparison of markov and quantum models of decision-making. *Journal of Mathematical Psychology*, 53:423–433. *3 citations, pages 5, 12, and 28*

Busemeyer, J., Wang, Z., and Townsend, J. (2006b). Quantum dynamics of human decision-making. *Journal of Mathematical Psychology*, 50:220–241. *3 citations, pages 20, 22, and 24*

Central Intelligence Agency (2008). The CIA World Factbook. http://www.odci.gov/cia/publications/factbook/. *Cited on page 29*

Cialdini, R. B. and Goldstein, N. J. (2004). Social influence: compliance and conformity. *Annu Rev Psychol*, 55:591–621. *Cited on page 30*

Diederich, A. (1997). Dynamic stochastic models for decision making under time constraints. *Journal of Mathematical Psychology*, 41(3):260–274. *Cited on page 22*

Diederich, A. and Busemeyer, J. R. (2003). Simple matrix methods for analyzing diffusion models of choice probability, choice response time, and simple response time. *Journal of Mathematical Psychology*, 47(3):304–322. *5 citations, pages 5, 12, 22, 24, and 27*

Dong, D., Chen, C., Li, H., and Tarn, T.-J. (2008). Quantum reinforcement learning. *IEEE Transactions on Systems, Man, and Cybernetics, Part B (Cybernetics)*, 38(5):1207–1220. *Cited on page 11*

Edwards, W., Lindman, H., and Savage, L. (1963). Bayesian statistical inference for psychological research. *Psychological Review*, 70(3):193–242. *Cited on page 3*

Eisert, J., Wilkens, M., and Lewenstein, M. (1999). Quantum games and quantum strategies. *Phys. Rev. Lett.*, 83:3077–3080. *Cited on page 10*

Ellsberg, D. (1961). Risk, ambiguity, and the savage axioms*. *The Quarterly Journal of Economics*, 75(4):643–669. *Cited on page 3*

Epping, G. P. and Busemeyer, J. R. (2023). Using diverging predictions from classical and quantum models to dissociate between categorization systems. *Journal of Mathematical Psychology*, 112:102738. *Cited on page 5*

Epping, G. P., Kvam, P. D., Pleskac, T. J., and Busemeyer, J. R. (2023). Open system model of choice and response time. *Journal of Choice Modelling*, 49:100453. *Cited on page 10*

Fakhari, P., Rajagopal, K., Balakrishnan, S. N., and Busemeyer, J. R. (2013). Quantum Inspired Reinforcement Learning In Changing Environment. *New Mathematics and Natural Computation (NMNC)*, 9(03):273–294. *Cited on page 11*

Farhi, E. and Gutmann, S. (1998). Analog analogue of a digital quantum computation. *Phys. Rev. A*, 57:2403–2406. *4 citations, pages 12, 16, 17, and 58*

Feller, A. and Livine, E. R. (2017). Quantum surface and intertwiner dynamics in loop quantum gravity. *Phys. Rev. D*, 95:124038. *2 citations, pages 12 and 23*

Flache, A., Mäs, M., Feliciani, T., Chattoe-Brown, E., Deffuant, G., Huet, S., and Lorenz, J. (2017). Models of social influence: Towards the next frontiers. *Journal of Artificial Societies and Social Simulation*, 20(4):2. *Cited on page 33*

Franco, R. (2009). Quantum amplitude amplification algorithm: An explanation of availability bias. In Bruza, P., Sofge, D., Lawless, W., van Rijsbergen, K., and Klusch, M., editors, *Quantum Interaction*, pages 84–96, Berlin, Heidelberg. Springer Berlin Heidelberg. *Cited on page 11*

Granovskiy, B., Gold, J. M., Sumpter, D. J. T., and Goldstone, R. L. (2015). Integration of social information by human groups. *Topics in cognitive science*, 7(3):469–493. *15 citations, pages 6, 8, 11, 21, 28, 29, 30, 31, 33, 37, 40, 44, 45, 50, and 58*

Grover, L. K. (1996). A fast quantum mechanical algorithm for database search. In *Annual ACM Symposium on Theory of Computing*, pages 212–219. ACM. *2 citations, pages 12 and 16*

Grover, L. K. (1998). Quantum computers can search rapidly by using almost any transformation. *Phys. Rev. Lett.*, 80:4329–4332. *Cited on page 6*

Grover, L. K. (2001). From schrödinger's equation to the quantum search algorithm. *Pramana*, 56(2):333–348. *2 citations, pages 12 and 16*

Hameroff, S. and Penrose, R. (2014). Consciousness in the universe: A review of the 'orch or' theory. *Physics of Life Reviews*, 11(1):39–78. *Cited on page 4*

Hancock, T. O., Broekaert, J., Hess, S., and Choudhury, C. F. (2020a). Quantum choice models: A flexible new approach for understanding moral decision-making. *Journal of Choice Modelling*, 37:100235. *Cited on page 10*

Hancock, T. O., Broekaert, J., Hess, S., and Choudhury, C. F. (2020b). Quantum probability: A new method for modelling travel behaviour. *Transportation Research Part B: Methodological*, 139:165–198. *Cited on page 10*

Hubbard, J. (1963). Electron correlations in narrow energy bands. *Proceedings of the Royal Society A*, 276. *2 citations, pages 12 and 23*

Jiang, C., Pan, Y., Wu, Z.-G., Gao, Q., and Dong, D. (2022). Robust optimization for quantum reinforcement learning control using partial observations. *Phys. Rev. A*, 105:062443. *Cited on page 11*

Jiang, J. and Liu, X. (2022). A quantum cognition based group decision making model considering interference effects in consensus reaching process. *Computers & Industrial Engineering*, 173:108705. *Cited on page 12*

Kahneman, D. (2011). *Thinking, fast and slow*. First edition. New York: Farrar, Straus and Giroux. *Cited on page 3*

Khodadadi, A., Fakhari, P., and Busemeyer, J. R. (2014). Learning to maximize reward rate: a model based on semi-markov decision processes. *Frontiers in Neuroscience*, Volume 8 - 2014. *Cited on page 37*

Khrennikov, A. (2010). *Ubiquitous Quantum Structure: From Psychology to Finances*. Berlin: Springer. *3 citations, pages 5, 9, and 13*

Khrennikov, A., Ozawa, M., Benninger, F., and Shor, O. (2025). Coupling quantum-like cognition with the neuronal networks within generalized probability theory. *Journal of Mathematical Psychology*, 125:102923. *Cited on page 4*

Khrennikov, A. Y. (2023). *Open Quantum Systems in Biology, Cognitive and Social Sciences*. Springer Cham. *2 citations, pages 5 and 10*

Khrennikova, P., Haven, E., and Khrennikov, A. (2014). An application of the theory of open quantum systems to model the dynamics of party governance in the us political system. *International Journal of Theoretical Physics*, 53:1346–1360. *Cited on page 10*

Kvam, P., Pleskac, T., Yu, S., and Busemeyer, J. (2015). Interference effects of choice on confidence: Quantum characteristics of evidence accumulation. *Proceedings of the National Academy of Sciences*, 112:10645–10650.

2 citations, pages 10 and 12

Lambert Mogiliansky, A., Zamir, S., and Zwirn, H. (2009). Type indeterminacy: A model of the kt(kahneman–tversky)-man. *Journal of Mathematical Psychology*, 53(5):349–361. Special Issue: Quantum Cognition. *Cited on page 5*

Li, J.-A., Dong, D., Wei, Z., Liu, Y., Pan, Y., Nori, F., and Zhang, X. (2020). Quantum reinforcement learning during human decision-making. *Nature Human Behaviour*, 4(3):294–307. *Cited on page 11*

Lyon, A. and Pacuit, E. (2013). *The Wisdom of Crowds: Methods of Human Judgement Aggregation*, pages 599–614. Springer New York, New York, NY. *Cited on page 33*

Maddison, C. J., Tarlow, D., and Minka, T. (2014). A∗ sampling. In Ghahramani, Z., Welling, M., Cortes, C., Lawrence, N., and Weinberger, K., editors, *Advances in Neural Information Processing Systems*, volume 27. Curran Associates, Inc. *Cited on page 37*

Martínez-Martínez, I. (2014). A connection between quantum decision theory and quantum games: The hamiltonian of strategic interaction. *Journal of Mathematical Psychology*, 58:33–44. *Cited on page 10*

Martínez-Martínez, I. and Sánchez-Burillo, E. (2016). Quantum stochastic walks on networks for decision-making. *Scientific Reports*, 6:23812. *Cited on page 10*

Moussaïd, M., Kämmer, J. E., Analytis, P. P., and Neth, H. (2013). Social influence and the collective dynamics of opinion formation. *PLoS One*, 8(11):e78433. *Cited on page 33*

Pothos, E. M. and Busemeyer, J. R. (2009). A quantum probability explanation for violations of 'rational' decision theory. *Proceedings. Biological sciences*, 276(1665):2171–2178. *2 citations, pages 10 and 20*

Pothos, E. M., Waddup, O. J., Kouassi, P., and Yearsley, J. M. (2021). What is rational and irrational in human decision making. *Quantum Reports*, 3(1):242–252. *Cited on page 4*

Rajagopal, K., Zhang, Q., Balakrishnan, S. N., Fakhari, P., and Busemeyer, J. R. (2021). *Quantum Amplitude Amplification for Reinforcement Learning*, pages 819–833. Springer International Publishing, Cham. *Cited on page 11*

Roland, J. and Cerf, N. J. (2003). Quantum-circuit model of hamiltonian search algorithms. *Physical Review A*, 68(6):062311–0623116. *2 citations, pages 12 and 16*

Rosner, A., Basieva, I., Barque-Duran, A., Glöckner, A., von Helversen, B., Khrennikov, A., and Pothos, E. M. (2022). Ambivalence in decision making: An eye tracking study. *Cognitive Psychology*, 134:101464. *Cited on page 10*

Shafir, E. and Tversky, A. (1992). Thinking through uncertainty: nonconsequential reasoning and choice. *Cogn. Psychol.*, 24:449–474. *Cited on page 3*

Sherif, M., Taub, D., and Hovland, C. (1958). Assimilation and contrast effects of anchoring stimuli on judgments. *Journal of Experimental Psychology*, 55(2):150–155. *Cited on page 33*

Simon, H. A. and Barnard, C. I. (1947). *Administrative behavior : a study of decision-making processes in administrative organization*. Macmillan Co., New York. *Cited on page 3*

Smith, P. and Ratcliff, R. (2015). An introduction to the diffusion model of decision making. *In B. U. Forstmann & E.-J. Wagenmakers (Eds.), An introduction to model-based cognitive neuroscience, New York, NY, US: Springer Science + Business Media.*, pages 49–70. *Cited on page 5*

Thaler, R. and Johnson, E. (1992). Gambling with the house money and trying to break even: The effects of prior outcomes on risky choice. *Management Science*, 36:643–766. *Cited on page 3*

Trueblood, J. and Busemeyer, J. (2011). A quantum probability account of order effects in inference. *Cognitive Science*, 35:1518–1552. *Cited on page 5*

Tversky, A. and Kahneman, D. (1983). Extensional versus intuitive reasoning: The conjunction fallacy in probability judgment. *Psychological Review*, 90:293–315. *Cited on page 5*

Tversky, A. and Shafir, E. (1992). The disjunction effect in choice under uncertainty. *Psychological Science*, 3(5):305–310. *2 citations, pages 3 and 5*

Wang, Z. and Busemeyer, J. R. (2016). Interference effects of categorization on decision making. *Cognition*, 150:133–149. *Cited on page 10*

Wang, Z., Solloway, T., Shiffrin, R. M., and Busemeyer, J. (2014a). Context effects produced by question orders reveal quantum nature of human judgments. *Proceedings of the National Academy of Sciences*, 111(26):9431–9436. *Cited on page 9*

Wang, Z., Solloway, T., Shiffrin, R. M., and Busemeyer, J. R. (2014b). Context effects produced by question orders reveal quantum nature of human judgments. *Proceedings of the National Academy of Sciences*, 111(26):9431–9436. *Cited on page 5*

Weinberg, S. (1995). *The Quantum Theory of Fields*, volume 1. Cambridge University Press. *Cited on page 19*

White, L. C., Pothos, E. M., and Busemeyer, J. R. (2014). Sometimes it does hurt to ask: The constructive role of articulating impressions. *Cognition*, 133(1):48–64. *Cited on page 9*

Yearsley, J. (2017). Advanced tools and concepts for quantum cognition: A tutorial. *Journal of Mathematical Psychology*, 78:24–39. *Cited on page 13*

Yearsley, J. and Busemeyer, J. (2016). Quantum cognition and decision theories: A tutorial. *Journal of Mathematical Psychology*, 74:99–116. *Cited on page 13*

Zheng, R., Busemeyer, J. R., and Nosofsky, R. M. (2023). Integrating categorization and decision-making. *Cogn Sci*, 47(1):e13235. *2 citations, pages 10 and 20*

Appendix A. Markov vs Schrödinger dynamics

	Markov	Schrödinger
State vector	$\Pi = \begin{pmatrix} p_1 \\ \vdots \end{pmatrix}$	$\psi = \begin{pmatrix} \psi_1 \\ \vdots \end{pmatrix}$
Vector components	probabilities, $\in \mathbb{R}$	probability amplitudes, $\in \mathbb{C}$
Entity’s state	$(0 \cdots 1_j \cdots 0)$	$(r_1 e^{i\theta_1} \cdots r_j e^{i\theta_j} \cdots r_N e^{i\theta_N})$
	“always at some single j"	“at j only after pos. meas. for j”
Normalization	$\sum_j p_j = 1$	$\sum_j \lvert\psi_j\rvert^2 = 1$
Propagator	$T(t) = e^{Kt}$	$U(t) = e^{-iHt}$
	$\sum_i T_{ij} = 1$	$U^\dagger U = I$
Change operator	Transition rate matrix K	Hamiltonian H
	$\sum_i K_{ij} = 0$, $K_{ij} \geq 0$, $i \neq j$	$H^\dagger = H$
Dynamics	$\Pi(t) = T(t)\Pi(0)$	$\psi(t) = U(t)\psi(0)$
Measurement for j	component selector M_j for j	subspace projector M_j for j
Probability for j	$\lvert\lvert M_j \Pi(t) \rvert\rvert_1$	$\lvert\lvert M_j \psi \rvert\rvert^2$

Table A.3: Comparison of the main model features in Markov and Quantum-like approach

Appendix B. Response data variation for trivia experiment

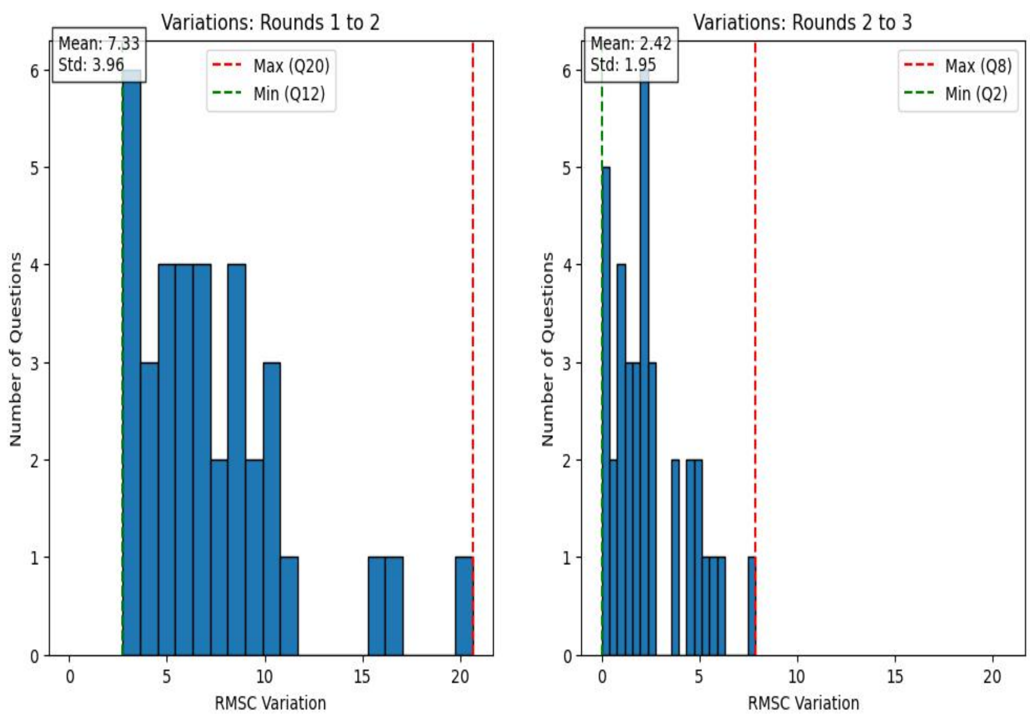

Figure B.6: Choice variation over rounds and questions, RMS of response change in 2nd round (left panel), and 3rd round (right panel). On average over questions, larger decision changes occur in the 2nd round in comparison to the third round.

Appendix C. Complex target design for belief state morphing

The basic morphing dynamics evolves the *source* to the *target*, Eq.(9), the former representing the subject's prior beliefs and the latter a **potentially multi-component** target belief state. From a cognitive modeling perspective on multi-respondent decision making, a variety of component-targets can be put forward and can be aggregated into a single target expression. In the supposition that some n distinct component-targets could be of interest, an

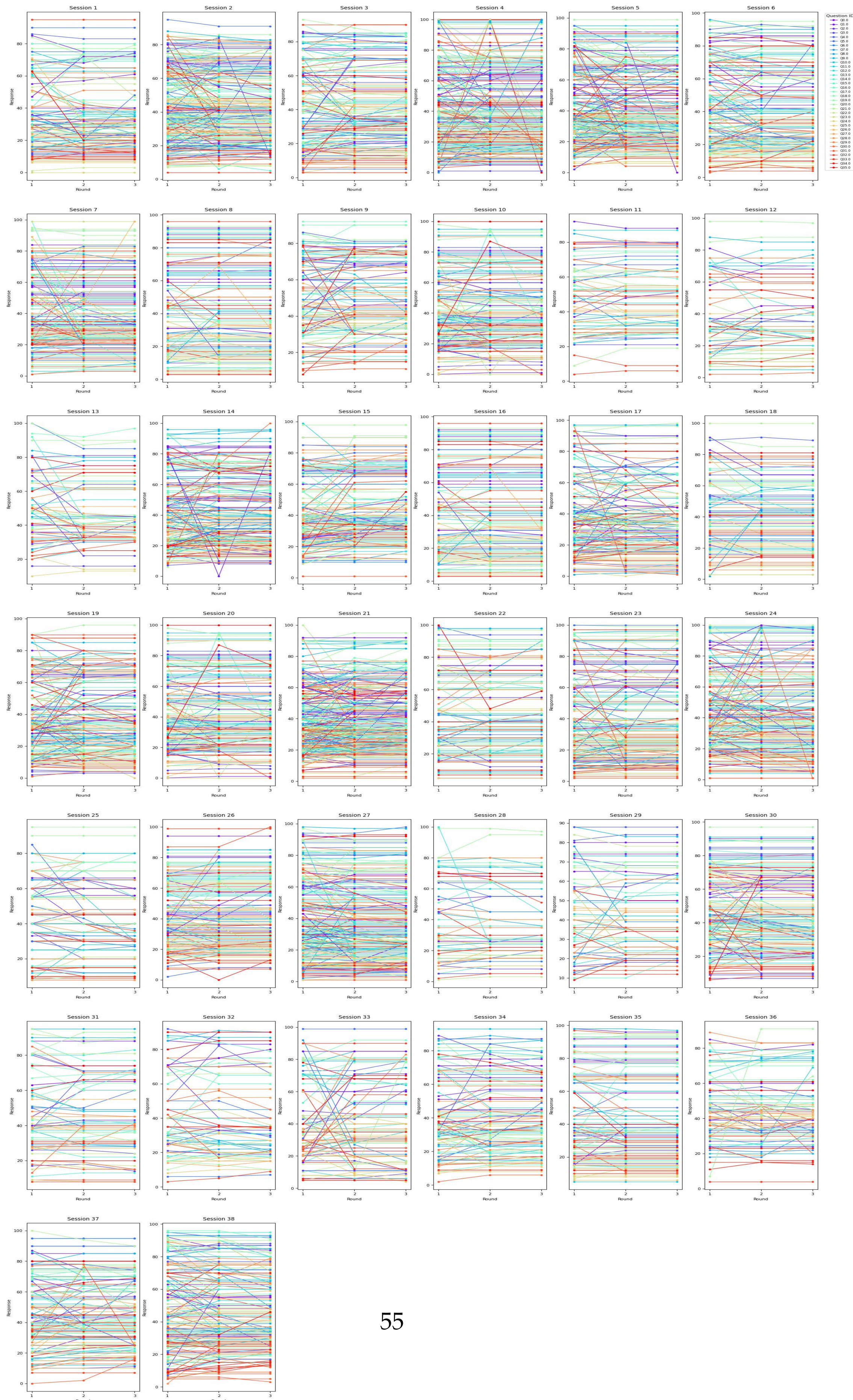

Figure B.7: Participant responses over question, rounds, and sessions.

aggregated single target state can be constructed which itself is the result of one source-state and a single target-state which is now the aggregate of the remaining $(n - 1)$ component-targets. This procedure can be repeated till the last target-state is the morphed state of one source-state and one single-component target-state:

$$\begin{aligned}
\psi_{X_0(\underbrace{\cdots}_{n\,\text{times}})} &= \cos(\rho_{X_0(X_1(\cdots))}t_0)\psi_{X_0} + ie^{-i\theta_{X_0(X_1(\cdots))}}\sin(\rho_{X_0(X_1(\cdots))}t_0)\psi_{X_1(\underbrace{\cdots}_{n\text{-}1\,\text{times}})} \\
&\cdots \\
\psi_{X_{n-1}(X_n)} &= \cos(\rho_{X_{n-1}(X_n)}t_{n-1})\psi_{X_{n-1}} + ie^{-i\theta_{X_{n-1}(X_n)}}\sin(\rho_{X_{n-1}(X_n)}t_{n-1})\psi_{X_n}
\end{aligned} \tag{C.1}$$

where $\rho_{X(\cdots)}$ and $\theta_{X(\cdots)}$ are the moduli and complex phases of the respective source-target inner products. The description of an n-component target-state in general requires n morphing strength parameters $\{t_0, \cdots, t_{n-1}\}$. From the aggregation process, Eq.(C.1), following a *linear binary tree* - i.e. a 3-regular tree graph - it can be seen that each subsequent target ψ_{X_i} is reached for t_j=$\tau_{j(j+1)}$ when $0 \leq j < i$ and t_i=0.

In an unbiased approach the target state can be left unspecified except for the inclusion of the elementary target belief states spanning its morphing space. By changing the n evolution parameters either of the n pure elementary targets can be reached from the initial belief. This morphing structure is a tree graph, with the initial belief being the root, vertices $v = n + 1$. The internal nodes are morphs that have degree 3 stemming from the parent morph and two child nodes. The leaves are the pure target belief states. Also, mixtures of these elementary belief states may compose the target

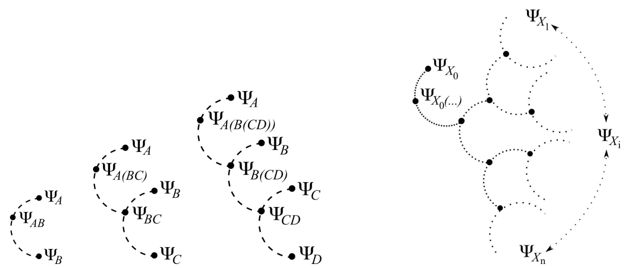

Figure C.8: Multi-target belief state morphing with 1, 2 and 3 components, ψ_{AB}, $\psi_{A(BC)}$ and $\psi_{A(B(CD))}$(left), and n components obtained from any 3-regular tree graph of targets $\psi_{X_0(1\cdots i\cdots n)}$ (right). Individual components can be reached by tuning the morph parameters, e.g. in the 3-components target; $\alpha_{B(CD)}$=0 for ψ_B, $\alpha_{B(CD)}$=$2\pi/\rho_{B(CD)}$ and $\alpha_{CD=0}$ for ψ_C, and, $\alpha_{B(CD)}$=$2\pi/\rho_{B(CD)}$ and α_{CD}=$2\pi/\rho_{CD}$ for ψ_D.

belief state.[18]

Appendix C.1. Analytical morph propagator

With the Hamiltonian $H = \mathcal{I} - P_{\psi_A} - P_{\psi_B}$, expressed on the projectors, and the Taylor expansion of the unitary propagator $U(t)$=$\sum_{k=0} \frac{(\text{-}it)^k}{k!} H^k$, its closed-form analytical expression can be obtained. Observing, $H\left\{P_{\psi_A}, P_{\psi_B}\right\}$=$-|\lambda|^2\left(P_{\psi_A} + P_{\psi_B}\right)$ and $H\left(P_{\psi_A} + P_{\psi_B}\right)$=$-\left\{P_{\psi_A}, P_{\psi_B}\right\}$, all powers of the Hamiltonian, H^k, for $k \in \mathbb{N}$ can be written as

$$H^k \quad = \quad H + a_k\left\{P_{\psi_A}, P_{\psi_B}\right\} + s_k\left(P_{\psi_A} + P_{\psi_B}\right) \tag{C.2}$$

subject to the recurrence relation a_{k+2}=$1 + |\lambda|^2 a_k$, and its initial conditions a_0=a_1=0 and recurrence relation s_{k+2}=$-|\lambda|^2(1-s_k)$, and its initial conditions s_0=1, s_1=0.[19] Taking into account even (n) vs uneven (m) powers of the

[18]Notice that in these cases the full morphing periods $\tau_{j(j+1)}$ are derived from the inner product of the known component target states ψ_{X_j} and $\psi_{X_{j+1}}$. Parameters for states deeper down the binary aggregation tree are redundant when an earlier parameter is zero.

[19]The choice s_0=1 allows the consistent expression for H^k of Eq.(C.2) when k=0.

Hamiltonian, the coefficients in the Taylor series can be rendered explicit with $s_n{=}-|\lambda|^2\frac{1-|\lambda|^{n-2}}{1-|\lambda|^2}$ (even), $s_m{=}-|\lambda|^2\frac{1-|\lambda|^{m-1}}{1-|\lambda|^2}$ (uneven), $a_n{=}\frac{1-|\lambda|^n}{1-|\lambda|^2}$ (even), and $a_m{=}\frac{1-|\lambda|^{m-1}}{1-|\lambda|^2}$ (uneven). The closed form expression of the propagator then becomes

$$\begin{aligned} U(t) &= e^{-it}H + \frac{1}{1-|\lambda|^2}\left\{P_{\psi_A}, P_{\psi_B}\right\}\left(e^{-it} - \cos|\lambda|t + \frac{i}{|\lambda|}\sin|\lambda|t\right) \\ &\quad - \frac{|\lambda|^2}{1-|\lambda|^2}\left(P_{\psi_A} + P_{\psi_B}\right)\left(e^{-it} - \frac{1}{|\lambda|^2}\cos|\lambda|t + \frac{i}{|\lambda|}\sin|\lambda|t\right), \end{aligned} \tag{C.3}$$

showing the simple addition of a phase e^{-it} outside the span of ψ_A and ψ_B, and a pure morphing within their span, and generalizes Farhi and Gutmann (1998)'s expression for the Grover-evolution of states in a 2D sub-space. The further simplified form, with $H{=}1-P_{\psi_A}-P_{\psi_B}$ absorbed, appears in Eq.(11). For completeness, the endmost cases are mentioned; i) when the source and target belief state are orthogonal, $\psi_A \perp \psi_B$ hence $\lambda{=}0$, the propagator reduces to $U(t){=}e^{-it}H + P_{\psi_A} + P_{\psi_B}$ –applying a phase only outside their span, and ii) when the source and target belief state coincide, $\psi_A{=}\psi_B$ hence $\lambda{=}1$, the propagator becomes $U(t){=}e^{-it}(1-P_\psi)+e^{it}P_\psi$ –applying one phase on the vector and the opposite phase outside its span.

Appendix C.2. Belief compromise

The morphing dynamics, Eq.(9), has been applied to conform a stepwise iterative updating process in which respondents refer to previous beliefs of the other respondents, e.g. as in the Trivia experiment (Granovskiy et al., 2015). Instead of inserting time-dependency of the morphing Hamiltonian by updating the projection states at each increment of time, the target morph state itself can be defined as an (un)balanced superposition of the respective belief states, $\gamma \in [0,1]$,

$$\Gamma \;=\; \gamma\psi_A + i\sqrt{1-\gamma^2}e^{-i\theta}\psi_B, \tag{C.4}$$

with the inner product of source and target yielding;

$$\langle\psi_A|\Gamma\rangle = \mathscr{N} e^{i\tan^{-1}\frac{\rho\sqrt{1-\gamma^2}}{\gamma}}, \qquad \mathscr{N} = \sqrt{\gamma + \rho^2(1-\gamma^2)} \tag{C.5}$$

The compromising morph state is derived by substituting the scalar product values, Eq.(C.5), and target state, Eq.(C.4), in the generic morphing relation, Eq.(9),

$$\begin{aligned}\psi_A(t) \;=\; & \left(\cos(\mathscr{N}t) + i\gamma e^{-i\tan^{-1}\frac{\rho\sqrt{1-\gamma^2}}{\gamma}}\sin(\mathscr{N}t)\right)\psi_A \\ & -ie^{-i\left(\theta+\tan^{-1}\frac{\rho\sqrt{1-\gamma^2}}{\gamma}\right)}\sqrt{1-\gamma^2}\sin(\mathscr{N}t)\psi_B,\end{aligned} \tag{C.6}$$

where phase θ and modulus ρ are again obtained from the inner product of the respective belief states, Eq.(6).

Appendix C.3. Belief polarization

The cognitive morphing dynamics can be adapted to evolve a belief state ψ_A to maximally differ with another given belief state ψ_B. The 'polarization' state χ of belief state ψ_A with respect to ψ_B satisfies: $\chi \perp \psi_B$ and $max\chi\langle\chi|\psi_A\rangle$. Any belief state can be decomposed into a parallel and orthogonal state w.r.t a second state, e.g. ψ_A=$P_B\psi_A + (1-P_B)\psi_A$. We define the 'polarization' target as the ψ_A-component orthogonal to ψ_B;

$$\chi \;=\; \frac{(1-P_B)\psi_A}{\mathscr{N}} \;=\; \frac{\psi_A - \lambda^\star \psi_B}{\mathscr{N}}, \tag{C.7}$$

where $|\chi|^2{=}1$, requires $\mathscr{N}{=}\sqrt{1-\rho^2}$. In this configuration the source-target scalar product satisfies $\langle\psi_A|\chi\rangle{=}\mathscr{N}$, and is real-valued. The polarization morph state is then obtained from the generic morphing relation, Eq.9,

$$\psi_A(t) \;=\; \left(\cos(\mathscr{N}t) + \frac{i}{\mathscr{N}}\sin(\mathscr{N}t)\right)\psi_A - i\frac{\lambda^\star}{\mathscr{N}}\sin(\mathscr{N}t)\psi_B, \tag{C.8}$$

which yields the orthogonal state $i\chi$ at $t{=}\tau_{\psi_A\chi}{=}\pi/(2\mathscr{N})$.

Appendix D. Gumbel sampling

For the expression of individual responses when no additional personal features of respondents are available, a small random variation about the response value with maximal probability in the updated belief state is implemented through Gumbel sampling. For a given belief state probability distribution pdf, the sampling $response$ is given by

$$logits = np.log(pdf) \tag{D.1}$$

$$noise = np.random.gumbel(size = len(logits)) \tag{D.2}$$

$$response = np.argmax(logits + noise/temperature) \tag{D.3}$$

in Python code. Sampling at a higher temperature mostly reduces the outcome to the unperturbed argmax of the belief state probability distribution, low-temperature sampling can veer the outcome to off-max response values by SD-size difference, Fig.D.9. To retain an acceptable level of model-fidelity, the lower limit of the Gumbel sampling temperature is set to T=20. The MAE-performance of the tested models depends on the applied Gumbel temperature, Fig.D.10. The performance mostly improves and converges with lower Gumbel temperature over the tested range $\{.2, 2, 20, 200, 2000\}$. The over-exploration at lower temperatures shows all models collapse to virtually the same performance level, confirming the requirement of the lower bound on the sampling temperature.The lower temperature sampling increases the performance through repeated trial-and-error sampling for each tested t_{frac}.

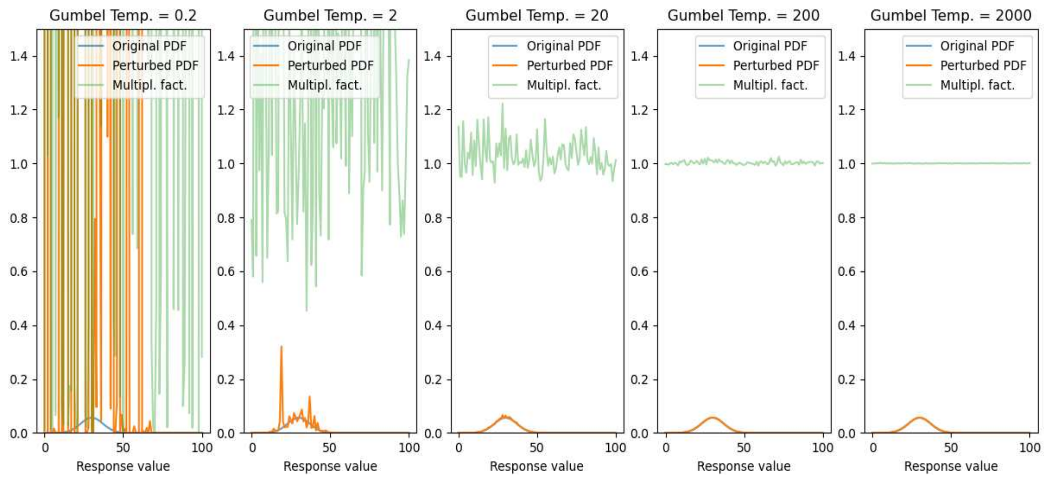

Figure D.9: Temperature vs response exploration; e.g. temperature's effect on Gumbel sampling for a belief probability distribution about response '30', with uncertainty SD=10.

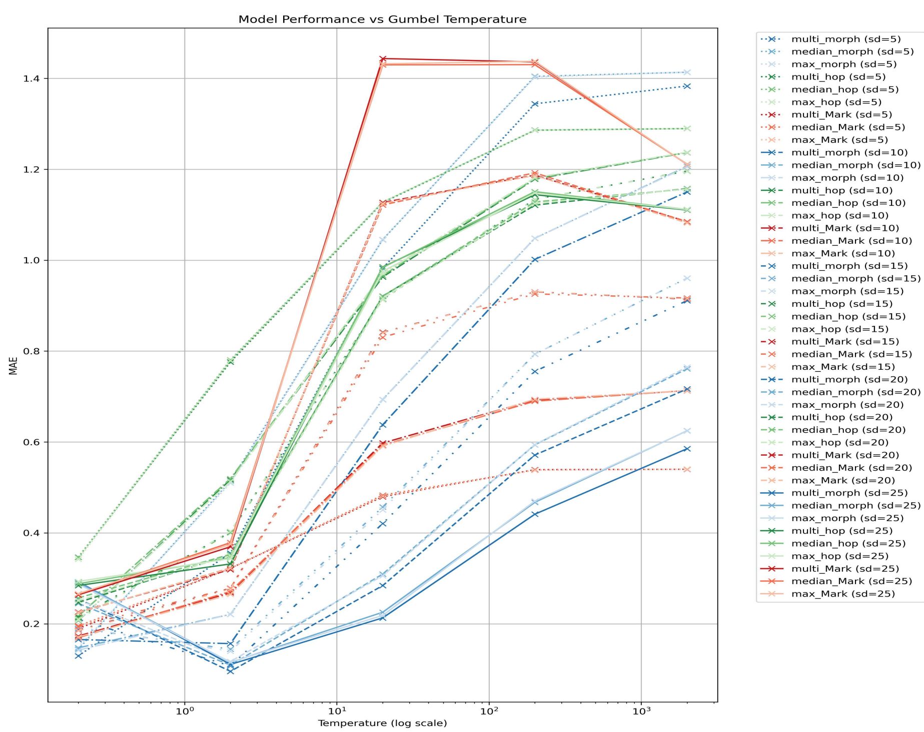

Figure D.10: Model MAE performance vs Gumbel temperature. All quantum and Markov models with *multi*, *median*, and *max* targets are tested with uncertainty SD=5 to 25, and sampling temperature T=.2 to 2000.